



THE UNIVERSITY *of* EDINBURGH

Edinburgh Research Explorer

The Broad-Spectrum Antimicrobial Potential of [Mn(CO)₄S₂CNMe(CH₂CO₂H)], a Water-Soluble CO-Releasing Molecule (CORM-401): Intracellular Accumulation, Transcriptomic and Statistical Analyses, and Membrane Polarization

Citation for published version:

Wareham, L, McLean, S, Beqq, R, Rana, N, Ali, S, Kendall, J, Sanguinetti, G, Mann, B & Poole, R 2018, 'The Broad-Spectrum Antimicrobial Potential of [Mn(CO)₄S₂CNMe(CH₂CO₂H)], a Water-Soluble CO-Releasing Molecule (CORM-401): Intracellular Accumulation, Transcriptomic and Statistical Analyses, and Membrane Polarization', *Antioxidants and Redox Signaling*, vol. 28, no. 14. <https://doi.org/10.1089/ars.2017.7239>

Digital Object Identifier (DOI):

[10.1089/ars.2017.7239](https://doi.org/10.1089/ars.2017.7239)

Link:

[Link to publication record in Edinburgh Research Explorer](#)

Document Version:

Peer reviewed version

Published In:

Antioxidants and Redox Signaling

General rights

Copyright for the publications made accessible via the Edinburgh Research Explorer is retained by the author(s) and / or other copyright owners and it is a condition of accessing these publications that users recognise and abide by the legal requirements associated with these rights.

Take down policy

The University of Edinburgh has made every reasonable effort to ensure that Edinburgh Research Explorer content complies with UK legislation. If you believe that the public display of this file breaches copyright please contact openaccess@ed.ac.uk providing details, and we will remove access to the work immediately and investigate your claim.



Antioxidants & Redox Signaling

Antioxidants & Redox Signaling: <http://mc.manuscriptcentral.com/liebert/ARS>

The Broad-Spectrum Antimicrobial Potential of [Mn(CO)₄(S₂CNMe(CH₂CO₂H))], a Water-Soluble CO-Releasing Molecule (CORM-401): Intracellular Accumulation, Transcriptomic and Statistical Analyses, and Membrane Polarization

Journal:	<i>Antioxidants and Redox Signaling</i>
Manuscript ID	ARS-2017-7239.R1
Manuscript Type:	Original - Rebound
Date Submitted by the Author:	n/a
Complete List of Authors:	Wareham, Lauren; Massachusetts Hospital and Harvard Medical School, Anesthesia, Critical Care and Pain Medicine; University of Sheffield, Molecular Biology and Biotechnology McLean, Samantha; Nottingham Trent University, School of Science and Technology; The University of Sheffield, Molecular Biology and Biotechnology Begg, Ronald; University of Edinburgh, School of Informatics Rana, Namrata; The University of Sheffield, Molecular Biology and Biotechnology Ali, Salar; The University of Sheffield, Molecular Biology and Biotechnology Kendall, John; Isogenica Ltd, ; The University of Sheffield, Molecular Biology and Biotechnology Sanguinetti, Guido; University of Edinburgh, School of Informatics Mann, Brian; University of Sheffield, Department of Chemistry Poole, Robert; The University of Sheffield, Molecular Biology & Biotechnology
Keyword:	Carbon monoxide, Infection, Metabolism, Metals, Microarray, Microbes, Models & Methods, Oxygen
Manuscript Keywords (Search Terms):	antibacterial agents, carbon monoxide-releasing molecule, manganese carbonyl compound, systems biology, uncoupling agent

SCHOLARONE™
Manuscripts

ORIGINAL RESEARCH - REBOUND TRACK

The Broad-Spectrum Antimicrobial Potential of [Mn(CO)₄(S₂CNMe(CH₂CO₂H))], a Water-Soluble CO-Releasing Molecule (CORM-401): Intracellular Accumulation, Transcriptomic and Statistical Analyses, and Membrane Polarization

Lauren K Wareham^{1*}, Samantha McLean¹⁴, Ronald Begg², Namrata Rana¹, Salar Ali¹, John J Kendall^{1§}, Guido Sanguinetti², Brian E Mann³, and Robert K Poole¹

¹Department of Molecular Biology and Biotechnology, The University of Sheffield, Sheffield, United Kingdom.

²School of Informatics, The University of Edinburgh, Edinburgh, United Kingdom.

³Department of Chemistry, The University of Sheffield, Sheffield, United Kingdom.

⁴School of Science and Technology, Nottingham Trent University, Nottingham, United Kingdom.

**Current affiliation:* Massachusetts General Hospital, Department of Anesthesia, Critical Care and Pain Medicine, Harvard Medical School, Boston, Massachusetts.

§ Current affiliation: Isogenica Ltd, Chesterford Research Park, Little Chesterford, United Kingdom

Correspondence to: Professor Robert K Poole, Department of Molecular Biology and Biotechnology, The University of Sheffield, Sheffield, S10 2TN, UK. Telephone: (+44) 114 222 4447; E-mail: r.poole@sheffield.ac.uk

Wareham: Antibacterial activities of a manganese CORM

Manuscript keywords: antibacterial agents, carbon monoxide-releasing molecule, manganese carbonyl compound, systems biology, uncoupling agent

Running head: Antibacterial activities of a manganese CORM (45)

Number of references: 75

Number of greyscale illustrations: 11

Number of color illustrations: 3 (online only)

Number of Supplementary illustrations: 4 (1 color, online only)

Number of Tables: 1

Number of Supplementary Tables: 1

Word count (Introduction to Discussion inclusive): 7,500

Sponsoring Peers: *Miguel Aon, Giancarlo Biagini, James Imlay, Nigel Robinson* (see Review

Comments in shaded box)

Abstract

Aims: Carbon monoxide (CO)-releasing molecules (CORMs) are candidates for animal and antimicrobial therapeutics. We aimed to probe the antimicrobial potential of a novel manganese CORM. **Results:** $[\text{Mn}(\text{CO})_4\text{S}_2\text{CNMe}(\text{CH}_2\text{CO}_2\text{H})]$, CORM-401, inhibits growth of *Escherichia coli* and several antibiotic-resistant clinical pathogens. CORM-401 releases CO that binds oxidases *in vivo* but is an ineffective respiratory inhibitor. Extensive CORM accumulation (assayed as intracellular manganese) accompanies antimicrobial activity. CORM-401 stimulates respiration, polarizes the cytoplasmic membrane in an uncoupler-like manner and elicits loss of intracellular potassium and zinc. Transcriptomics and mathematical modeling of transcription factor activities reveal a multifaceted response characterized by elevated expression of genes encoding potassium uptake, efflux pumps, and envelope stress responses. Regulators implicated in stress responses (CpxR), respiration (Arc, Fnr), methionine biosynthesis (MetJ) and iron homeostasis (Fur) are significantly disturbed. Although CORM-401 reduces bacterial growth in combination with cefotaxime and trimethoprim, fractional inhibition studies reveal no interaction. **Innovation:** We present the most detailed microbiological analysis yet of a CORM that is not a ruthenium carbonyl. We demonstrate CO-independent, striking effects on the bacterial membrane and global transcriptomic responses. **Conclusions:** CORM-401, contrary to our expectations of a CO delivery vehicle, does not inhibit respiration. It accumulates in the cytoplasm, acts like an uncoupler in disrupting cytoplasmic ion balance, and triggers multiple effects including osmotic stress and futile respiration. **Rebound Track:** This work was rejected during standard peer review and rescued by Rebound Peer Review (*Antioxid Redox Signal* 16:293-296, 2012) with the following serving as open reviewers: Miguel Aon, Giancarlo Biagini, James Imlay, Nigel Robinson.

Wareham: Antibacterial activities of a manganese CORM

1
2
3
4
5
6
7
8
9
10
11
12
13
14
15
16
17
18
19
20
21
22
23
24
25
26
27
28
29
30
31
32
33
34
35
36
37
38
39
40
41
42
43
44
45
46
47
48
49
50
51
52
53
54
55
56
57
58
59
60

CONFIDENTIAL. For Peer Review Only

Introduction

There is an urgent need for new antimicrobial agents; carbon monoxide (CO) - a poisonous, gas that avidly binds to ferrous hemes in globins and oxidases inhibiting respiration (29) may, in principle, be a potent antimicrobial molecule. However, CO also plays essential physiological roles (35) as a gasotransmitter (50) (or ‘small molecule signaling agent’ (18)). CO is endogenously produced by heme oxygenase that catalyzes the degradation of heme, liberating CO, which then modulates key anti-inflammatory, anti-apoptotic and cytoprotective effects. However, the handling and health risks associated with administering CO gas have prompted the design and administration of CO-releasing molecules (CORMs), predominantly metal carbonyl compounds, allowing substantial advances in the biochemistry and physiology of CO (8,37). Diverse CORMs differ in structure, kinetics and in CO release mechanisms (70).

The first water-soluble CORM to be

Rebound Track

This work was rejected during standard peer review and rescued by Rebound Peer Review (*Antioxid Redox Signal* 16:293-296, 2012) with the following serving as open reviewers: Miguel Aon, Giancarlo Biagini, James Imlay, Nigel Robinson. The comments by these reviewers supporting the rescue are listed below:

Miguel Aon (miguel.aon@nih.gov): I am a qualified reviewer (per *Antioxid Redox Signal* 16:293-296) and move to rescue this article that was rejected during the regular peer review process after reviewing all versions of the article and detailed reviewer comments. The manuscript entitled *The Broad-Spectrum Antimicrobial Potential of [Mn(CO)₄(S₂CNMe(CH₂CO₂H))], a Water-Soluble CO-Releasing Molecule (CORM-401): Intracellular Accumulation, Transcriptomic and Statistical Analyses, and Membrane Polarization* represents a comprehensive, in-depth assessment of the antibiotic function of CORM-401, a carbon monoxide-releasing, manganese-

Wareham: Antibacterial activities of a manganese CORM

synthesized and used biologically - based compound. The most important scientific contribution of this work is the detailed assessment of the mechanism of action of CORM-401 to inhibit the growth of bacteria. The emerging picture is of a pleiotropic nature, with multiple targets that functionally converge on adverse bioenergetic effects hindering bacterial growth. As a former Invited Forum Editor and Author of *Antioxidant & Redox Signaling* I clearly understand and adhere to the Journal's policy of scientific excellence. In this vein, I am confident that the work by Wareham and colleagues fits those standards while making a remarkable scientific contribution. The few questions/concerns raised by the Reviewers are not of enough scientific substance to reject sound work based on a substantial and comprehensive amount of evidence. The key issue from this work is that perturbations of the proton motive force elicited by CORM-401 are matched by enhanced respiration leading to membrane polarization, which in turn drives the uptake of CORM-401 by bacteria, poisoning them by its intracellular accumulation. This seminal effect facilitates the intracellular action of CORM-401 on multiple targets leading to growth arrest. Therefore in the interests of science,

Rigorous bacterial chemostat experiments involving transcriptomic datasets and mathematical modeling have revealed unexpected aspects of CORM-3 biochemistry. First, diverse biological processes are affected by CORM-3, not only respiratory function (38). Second, CORM-2 and CORM-3 elicit effects that cannot be mimicked by CO gas, even at concentrations much higher than the ruthenium (Ru) CORMs (73). Third, even CO-depleted control molecules (so-called 'inactive CORM-3', iCORM) modulate bacterial gene expression, despite the inability to detect significant CO release from such molecules in the myoglobin assay (38). Finally, although heme is

the classical target of CO in biological chemistry, heme-deficient bacteria are also sensitive to CORM-3 and display complex patterns of gene expression in response to this compound (74).

In view of the potential importance of CORMs as antibacterial agents, and the mounting evidence for involvement of the metal and co-ligand fragment of CORMs in their biological effects (38,74), we have used a newer compound that lacks Ru, a biologically ‘foreign’ molecule. $[Mn(CO)_4S_2CNMe(CH_2CO_2H)]$, CORM-401, is a CO-releasing manganese complex providing up to 3.2 moles CO per mole of compound (7), depending upon the concentration of the CO acceptor myoglobin and the presence of oxidants (16). The mechanism of CO loss is dissociative and reversible; reversible binding of CO results in a relatively stable solution of the compound (7).

Here we present the most detailed microbiological analysis to date of a non-Ru CORM and contrast its effects with the potent actions of CORMs-2 and -3, whose actions are probably explicable in part by the biological chemistry of the accumulated Ru. Although less potent as an antibacterial agent, CORM-401 is extensively accumulated by bacteria,

I take full responsibility to rescue this work from rejection.

Giancarlo Biagini

(giancarlo.biagini@lstmed.ac.uk): I am a qualified reviewer (per *Antioxid Redox Signal* 16:293-296) and move to rescue this article that was rejected during the regular peer review process after reviewing all versions of the article and detailed reviewer comments. The manuscript investigates the mechanism of action of a CO-releasing molecule and describes biochemical, cellular bioenergetic and transcriptional responses of *E. coli* to CORM-401. The innovation of the manuscript is that these data are the first to describe the pharmacodynamics of this “second generation” CORM. The findings suggest a pleiotropic mechanism of action, which includes disruption of respiratory chain components and of membrane integrity in terms of ion transport/homeostasis. It is likely that the disruption of these two biological functions is linked. One of the referees questions the demonstration that CORM-401 stimulates respiration. However, this is clearly demonstrated in Fig 7. The experiments show the use of the open O₂ electrode, widely used and often in preference to

Wareham: Antibacterial activities of a manganese CORM

increases oxygen consumption and membrane polarization in an uncoupler-like fashion, and triggers myriad effects including osmotic and envelope stresses.

Results

CORM-401 releases CO under bacterial growth conditions

Medium or buffer composition and the presence of oxidants, reductants and a CO-acceptor (such as a heme protein) are important determinants of the rates and extent of CO loss from CORMs (16,39). We therefore characterized CO release from CORM-401 *in vitro* under our conditions using ferrous myoglobin assays in which maximum sensitivity was achieved by monitoring the Soret bands in CO difference spectra (39) (Fig. 1A). In defined (Evans) growth medium, at physiological temperature (37 °C) and pH (7.4), 2.5 mol equivalent of CO was released to myoglobin with a half-time of 4.5 min. In 0.1 M KPi buffer at 37 °C, the half-time was 5 min and the yield of CO was 2.4 mol/mol; at 20 °C, the rate was slower (Supplementary Fig. S1). Fayad-Kobeissi et al. (16)

the closed system as one has the ability to set the dissolved O₂ tension of the chamber, which clearly demonstrates stimulation of O₂ consumption following the introduction of CORM-401. The positive control experiment using KCN clearly indicates that the system is working normally. In vivo data are required in order to establish the development potential of molecules but, in this case, this investigation is first attempting to determine the molecular mechanisms underpinning the activity of this class of compounds. It is therefore not normal practice to conflate the two issues. Therefore in the interests of science, I take full responsibility to rescue this work from rejection.

James Imlay (jimlay@illinois.edu): I am a qualified reviewer (per *Antioxid Redox Signal* 16:293-296) and move to rescue this article that was rejected during the regular peer review process after reviewing all versions of the article and detailed reviewer comments. I have closely read the manuscript and the reviewers' comments. My overall reaction is that the manuscript is sound, and I advise that a decision be made to ACCEPT the paper. I was surprised by the outcome. I would

reported that the yield of CO increased as the myoglobin:CORM-401 ratio increased, with 2.6 mol observed at a ratio of 5:1. This is in close agreement with our values (Fig. 1B, Supplementary Fig. S1). Although sodium dithionite facilitates CO release from CORM-3, CORM-401 is able to release CO spontaneously in the absence of dithionite with oxyhemoglobin as a CO acceptor (39). The CO release kinetics in Fig. 1 demonstrate the rapid release from CORM-401 of CO in growth medium; whether CO is released prior to, during or after CORM uptake (see below), the gas will be available in the following bacterial experiments.

CORM-401 toxicity is dependent on the carbon source for growth

The effect on bacterial growth was determined by adding CORM-401 to mid-exponential phase cultures in replicate experiments (representative cultures are shown in Fig. 2A and B). CORM-401 slightly perturbed growth of cells on glucose at 67 μ M and significantly slowed growth only at 500 μ M (Fig. 2A). When CO is liberated from CORM-401, a Mn(II) salt and a dithiocarbamate (DTC) ligand remain. In minus-

have predicted that toxicity was mediated by the usual action of CO. The loss of viability in Fig. 2 was enough to alert me that I was wrong. This is nice work. A reviewer requested *in vivo analysis*, but because these compounds impact host cells, a study of CORM-401 impact in host animals would be large and complex. Another wrote: *authors should determine O₂ consumption rate*. This method is not new. Standard measurements of consumption (Fig. 7B) are problematic when rates are low. But in Figs. 7C and 7D the reader can immediately see that CORM-401 and CCCP cause an increase in oxygen consumption, as evidenced by the lower steady-state oxygen level. The same reviewer wrote: *oxygen consumption or even OCR could increase due to several processes other than respiration*. I disagree with the reviewer's suggestion that non-respiratory processes could accelerate oxygen consumption. *E. coli* lacks non-respiratory enzymes that employ molecular oxygen as a substrate, as this facultative bacterium must manage biosynthesis without oxygenases. Indeed, if one knocks out the respiratory oxidases, oxygen consumption essentially ceases. Therefore in the interests of science, I take full responsibility to

CO control experiments, a combination of Mn(II) sulfate and sarcosine DTC was added to final concentrations of 500 μ M with no deleterious effect on growth (Fig. 2A, inset).

We hypothesized that succinate-grown cells would be perturbed by CORM-401 to a greater extent than on glucose, due to physiological reliance on heme terminal oxidases that are inhibited by CO. Indeed, growth on succinate was inhibited to a greater extent by CORM-401 (Fig. 2B); unlike glucose-grown cells, cells failed to grow on succinate with 500 μ M CORM-401 (Fig. 2B). Although inhibition of oxidase function may contribute to this distinction, this manuscript reveals a multitude of effects on unrelated cellular functions. The control compounds again showed no deleterious effect on growth (Fig. 2B, inset). To dissect the effect of CO gas and the CORM, we tested the addition of a CO-saturated solution on growth of cell cultures. Due to limitations of CO solubility and the undesirability of adding large volumes of gas solutions to cultures, a final concentration of 100 μ M was used; no inhibition of growth was observed (data not shown), as shown before (69). Thus the observed effects of CORM-

rescue this work from rejection.

Nigel Robinson (nigel.robinson@durham.ac.uk): I am a qualified reviewer (per *Antioxid Redox Signal* 16:293-296) and move to rescue this article that was rejected during the regular peer review process after reviewing all versions of the article and detailed reviewer comments. Carbon monoxide-releasing molecules (CORMs) might be a new class of antimicrobials, with the looming threat of antimicrobial resistance making work to explore such options pertinent. Here, multiple approaches have explored facets of bacterial physiology (respiration, transport, membrane integrity) and molecular cell biology (including extensive expression profiling) to carefully tease apart the mechanism(s) of bacterial growth inhibition by CORM-401. The resulting observations do not mirror the effects of related ruthenium-containing CORMs, neither does exposure of cells to CO alone mimic the effects of CORM-401: these data thus point to features of the compound other than solely the liberated CO exerting inhibitory effects, with manganese as opposed to ruthenium, appearing to be one crucial distinction. The work is a *tour de force*; in short, the action of CORM-401

401 on growth are in part attributed to the metal co-ligand fragment of the compound and not the CO alone as previously supposed. Bactericidal activity of the compound was assessed by viable counts. Note, however, that there is no useful correlation between biomass as assessed by optical density (light scattering) measurements (Fig. 2A, B) and viable cell numbers as assessed by colony counting after dilutions (Figs. 2C, D). Light scattering certainly does not give information on the number of cells (17,32). Although glucose-grown cultures increased in total biomass at <100 μ M CORM-401, viability on agar decreased at 500 μ M after 2 h (Fig. 2C). In contrast, cells grown on succinate (Fig. 2D) retained viability on agar, even at 500 μ M CORM-401, despite a lack of increase in biomass (Fig. 2B). The apparent discrepancy in these two media might result, for example, from the clumping of cells in glucose (leading to an artefactually low cell count) or the ability of succinate-grown cells to retain viability after removal from the CORM, though being inhibited within the CORM-supplemented culture.

is multifaceted and includes CO-binding to respiratory oxidases but also manganese hyper-accumulation with effects on the homeostasis of other metals (such as zinc), ionic imbalance and loss of membrane integrity, and defined regulons. The extent of functional studies was questioned, yet the work is rich in a diversity of types of functional studies; these assays have demanded a high degree of technical skill in using a wide range of methodologies. Evidence that the compound stimulates respiration was questioned. However, bacterial respiration rates have been determined from measurements of oxygen concentrations and oxygen diffusion rates. Editorial comments note the lack of *in vivo* studies: it may be felt that ultimately the compound should be used in animal models of infection, but the modest effectiveness of this CORM as an antimicrobial agent suggests that animal studies are not justified (or perhaps ethical). Therefore in the interests of science, I take full responsibility to rescue this work from rejection.

CORM-401 accumulates to millimolar concentrations in the bacterial cytoplasm and binds DNA

We hypothesized that the loss of viability of glucose-grown cells (Fig. 2C) might be due to substrate-dependent differences in CORM uptake. CORMs-2 and -3 are accumulated by bacteria, as inferred from intracellular Ru concentrations (9,27,38). Therefore, intracellular accumulation of CORM-401 was measured using inductively-coupled plasma mass spectroscopy (ICP-MS) (38). However, the metal in CORM-401 is Mn, itself a component of all cells and so we sought elevated accumulation of this metal, relative to no-CORM controls. Cells growing on glucose or succinate in the presence of CORM-401 at two concentrations were assayed over time and concentrations of manganese were determined in cell pellets, using literature values for cell size and volume to estimate cellular concentrations.

When cells were grown on glucose with 67 μ M CORM-401, manganese was accumulated biphasically (Fig. 3A, closed circles), rapidly within 2.5 min, then more slowly over 80 min to reach an intracellular concentration of ~ 3.5 mM manganese. In contrast, uptake by succinate-grown cells was monophasic, reaching ~ 1.5 mM after 80 min (Fig. 3A, open circles). Thus, in glucose media, bacteria accumulate more CORM-401 (Fig. 3A). Since 500 μ M CORM-401 was needed to significantly slow growth, we also tested this concentration and assayed cell pellets after 80 min growth; in cells grown on glucose or succinate, the values found in cell pellets were 16.5 ± 0.69 mM and 10.9 ± 0.55 mM, respectively. The data sets are statistically different ($P < 0.05$). Thus, irrespective of the CORM concentration in media, bacteria accumulate more CORM-401 in glucose media and suffer reduced viability (Fig. 2C). Note, however, that most of the accumulated manganese will be bound and buffered such that the exchangeable concentration within living cells will be much lower than the maximum we recorded of 3.5 mM. Therefore, an apparent concentration of, say, 3.5 mM manganese is better expressed as 0.7×10^7 atoms/cell (see Methods).

To determine the fate of accumulated manganese, cultures exposed to 67 μ M CORM-401 were harvested and fractionated to give soluble, membrane, and genomic DNA fractions, which were retained and quantitatively analyzed for manganese by ICP-MS. As shown in Fig. 3B, manganese was found predominantly in the cytoplasm, but also in DNA. CORM-401 itself is unlikely to coordinate DNA but pyridine reacts to give $\text{Mn}(\text{CO})_3(\text{py})(\text{DTC})$, as observed by IR spectroscopy (7), suggesting that an N base in DNA could behave similarly. A protein histidine residue is a candidate for binding of CORM-3 (59).

It was important to define the active species of CORM-401; this might be CO released from the compound, the residual Mn(II) salt, or the dithiocarbamate (DTC) ligand. In the absence of CORM, the Mn levels of succinate-grown cells were higher than for glucose-grown cells (Fig. 3 C) (note the different ordinate scales in Figs. 3A, C and D). However, metal levels were not influenced by CO in solution, even at 500 μ M, after 80 min incubation. Adding MnSO_4 (500 μ M) increased the intracellular Mn levels, as expected, but a combination of MnSO_4 and DTC was without further effect. We conclude that the modest increases observed in the control experiments in Figs. 3C and D demonstrate that CORM-401, but not the control species (Mn, CO, DTC), significantly elevates intracellular Mn pools.

Exposure to CORM-401 leads to transient changes in transcription of multiple gene groups

The accumulation of CORM-401 to strikingly high levels and correlation with bacterial killing (Figs. 2, 3) prompted further analysis of the global responses to this CORM. We therefore conducted transcriptomic analyses on CORM 401-treated cells in glucose medium. The concentration of CORM selected (67 μ M) led to minor growth perturbation. Lethal concentrations of CORM were avoided: we sought transcriptomic responses to stress responses,

rather than cell death. CORM-401 altered expression of numerous genes in distinct classes (Fig. 4). Following standard practice, we retained for our initial analyses genes exhibiting a fold change ≥ 2 -fold up or ≥ 2 -fold down (the latter representing a change of ≥ 0.5 of the control transcript level). We then performed an in-depth analyses of the transcriptomic response using the statistical modelling approach of TFInfer.

The response was transient both aerobically and anaerobically. Aerobically, 23 % of the genome was significantly up- or down-regulated within 40 min (Fig. 4A). Anaerobically, although the magnitude of gene changes across many of the categories was smaller, and the response slightly delayed, the pattern in the response was again transient; at 40 min, gene changes were highest with 18 % of the entire genome changing (Fig. 4B).

Aerobically, the most marked changes were in genes involved in motility, and energy, carbohydrate and nucleotide metabolism (Fig. 4A). The most altered category was motility; after 40 min exposure to CORM-401 in aerobic conditions, 35 % of genes in this category were down-regulated, consistent with the compromised motility of cells treated with a solution of CO (38). However, we found that motility (swarming) of cells was not diminished by CORM-401 (see later). Energy metabolism genes were transiently affected by the addition of CORM-401 under aerobic conditions; genes were down-regulated progressively over time and reached a minimum at 20 min where 24 % of energy metabolism-related genes were down-regulated (Fig. 4A). Anaerobically, the gene categories most affected were those involved in energy metabolism, carbohydrate metabolism, phosphotransferase system genes (PTS) and motility (Fig. 4B). Genes involved in energy metabolism were more highly down-regulated anaerobically than aerobically (Fig. 4B, see later). Signal transduction genes and genetic information processing genes were highly up-regulated: 17 % of signal transduction genes were up-regulated after 20 min.

Genes are described subsequently according to their functional characteristics. However, Supplementary Table 1 presents a list of the thirty most highly up-regulated genes, both aerobically and anaerobically.

Modelling of transcriptomic data

To analyze the underlying transcription factors (TFs) responsible for the transcriptome data, we used TFInfer (2,57,69), a Bayesian statistical method that integrates gene expression data with regulon information (culled from Regulon DB or EcoCyc) to identify TF activity profiles that aid understanding of the raw transcriptional changes. We ran TFInfer separately on the CORM-401 (this work) and CO gas data sets (69) to identify differences in the magnitude and kinetics of the response to the two stimuli. Fig. 5 summarizes the differences between two sets of TFInfer data using “coherence plots” (introduced in (69)); the abscissa (x-coordinate) of each point (labeled with the TF identity) represents the ‘profile difference’ between the two conditions, computed as 1 minus the absolute Pearson correlation coefficient between the two profiles, while the ordinate (y-coordinate) represents the change in magnitude of the response (computed as the absolute difference of the norms of the two profiles). Hence, TFs whose response is similar both in magnitude and kinetics are located near the origin of the coherence plot, while TFs in the top right corner of the plot respond differently in both kinetics and amplitude.

In this analysis, we identified several key regulators whose activity underlies the effects described later. Thus, CpxR appears in quadrants ‘a’ of Fig. 5 (A, aerobic and B, anaerobic), hence exhibiting correlated temporal profiles but a large difference in response magnitude. CpxR is a member of the two-component regulatory system CpxA/CpxR that combats extra-

cytoplasmic protein-mediated toxicity by increasing the syntheses of the periplasmic protease DegP and CpxP protein. However, the response regulator Fis, which is involved in maintenance of nucleoid structure and other functions including biofilm formation, motility and chemotaxis, is in both quadrants 'c' of Fig. 5, indicating its response is similar in magnitude and kinetics when cells are exposed to CO gas or CORM-401 in aerobic or anaerobic conditions. As a further example of the correlation analysis, the coherence plot also reveals that FhlA (the transcriptional activator of the formate hydrogenlyase system, quadrant 'd' of Fig. 5, top, aerobic) responds similarly in terms of the activity profile when cells are exposed to CORM-401 or CO gas, but the magnitudes of the responses are dissimilar and FhlA does not appear in the anaerobic analysis. (Note that FlhA, required for flagellar biosynthesis, also appears in these analyses as a pertinent transcription factor, but its activity is little altered in the aerobic and anaerobic states.) Each point on the plot has both horizontal and vertical error bars associated with it, which take into account the uncertainty in the inferred TF activities derived from TFInfer. In Fig. 5, these error bars have been omitted to reduce visual clutter; error bars are shown in Supplementary Fig. S2.

CORM-401 perturbs respiratory gene expression

Energy metabolism was significantly altered, both aerobically and anaerobically, in response to CORM-401 (Fig. 4). The TFInfer coherence plot reveals two TFs that regulate genes in central respiratory metabolism: FNR (Fumarate Nitrate Reduction regulator) and ArcA. While Fnr was less perturbed (being in quadrant 'c' of Figs. 5A and B), ArcA responded differently under each condition (lying in quadrant 'd' of Fig. 5A but in quadrant 'c' of Fig. 5B). ArcAB, a two-component system, indirectly senses oxygen, in part via the redox state of the quinone pool (1). Under anoxic or microaerobic conditions, ArcB autophosphorylates, then

transphosphorylates ArcA through a phospho-relay, increasing the affinity of ArcA for its DNA targets (26). Phosphorylated, active ArcA (ArcA-P) then represses expression of genes involved in aerobic respiration (e.g. electron transport enzymes, cytochrome *bo'* and the Krebs cycle enzymes) and activates genes involved in fermentative metabolism and cytochrome *bd*. Thus, in a mutant lacking oxidase function, as in the absence of oxygen as electron acceptor, the aerobic expression of Arc-A-P-activated genes, like *cydAB*, is elevated, but that of ArcA-P-repressible genes, like *cyoABCDE* (encoding the heme-copper oxidase) is lowered (25) because the quinone pool is trapped in a reduced form and unable to inhibit the autokinase activity of ArcB.

Indeed, Fig. 6 shows that CORM-401 mimicked microaerobic/anaerobic conditions even in the presence of oxygen; it very strongly increased expression of *cydAB* (encoding cytochrome *bd-I*) presumably reflecting respiratory inhibition. Davidge *et al* also reported an increase in *cydAB* transcripts in response to CORM-3 (9). However, anaerobically, the *cydAB* genes were down-regulated after 5 min. In contrast, genes encoding the cytochrome *bo'*-type oxidase (*cyoABCDE*) were, under aerobic conditions, down-regulated by approximately 5-fold transiently after 5 min. This is consistent with repression of *cyo* expression by phosphorylated (active) ArcA. Anaerobically, the *cyo* operon was consistently down-regulated by CORM-401; *cyoA* was 10-fold down-regulated after 10 min. Fold changes relating to respiratory changes are given in Supplementary Fig. S3 A.

Fig. 6 also shows other respiratory genes. The *nuo* genes encode a multi-subunit, proton-translocating NADH dehydrogenase; all were up-regulated by CORM-401 under aerobic conditions together with the oxidase genes. The initial CORM-401-induced increases in *cyo* expression (0-5 min) and the sustained increase in *nuo* expression (0-80 min) under aerobic conditions are not consistent with the anticipated repression of these systems by Arc alone;

indeed, *nuo* expression is regulated in a complex fashion, not only by ArcA, but also NarL, Fnr, IHF and other factors including C₄ dicarboxylates (5). In contrast to the effects of CO gas (69), expression of *ndh*, encoding NADH dehydrogenase II, was up-regulated both aerobically and anaerobically for the first 5-10 min after CORM-401 exposure (Fig. 6).

CO released from CORM-401 is targeted to terminal oxidases in vivo

Changes in respiratory gene expression suggested interference with respiration, so we assessed CO targeting of the oxidases using spectrophotometry on intact cell suspensions. CO bound rapidly to terminal oxidases upon addition of 100 μ M CORM-401 (Fig. 7A). In the first scan, the 645 nm signal corresponds to the absorbance maximum of CO-ligated cytochrome *d*, and the 620 nm trough indicates removal of the ferrous cytochrome *d* from the difference spectrum (9,27). Subsequently, a peak at 412 nm appeared, suggesting slower binding of CO to cytochrome *o*. The developing trough at 442 nm has contributions from the ferrous hemes of cytochromes *o*, *d* and *b*₅₉₅ (27,56). More slowly formed were the α/β bands at 540 nm, 556 nm and 570 nm with contributions from multiple CO-reactive hemes. Thus, CO is released almost immediately upon addition to cells and is initially targeted to the cytochrome *bd*-type oxidase, coincident with up-regulation of *cydAB* transcripts in aerobic cells (Fig. 6, Supplementary Fig. A).

CORM-401 stimulates respiration

In view of the expected (29) and observed targeting of respiratory oxidases by CO released from CORM-401 (Fig. 6), we measured directly the effects of CORM-401 on respiration. Bacterial membranes were incubated in a chamber closed with a lid preventing

inwards diffusion of oxygen, so that oxygen consumption decreases dissolved oxygen.

Respiration was stimulated with 6.25 mM NADH and followed until ~75% air saturation (shown by the arrow in Fig. 7B), where 100 μ M CORM-401 or CO-saturated solution were added.

Under these conditions, CORM-401 inhibited membrane respiration by up to 32 % and equimolar CO gas inhibited respiration by up to 48 %. However, the periods of observation were limited by oxygen depletion from the chamber.

To allow longer observations on intact bacteria, in which the duration of the measurement is not limited by the amount of O₂ initially present in the liquid, we used the well-established 'open' system, allowing inward O₂ diffusion to balance oxygen consumption. In such a chamber (Fig. 7C) (10), the respiration rate at steady-state is proportional to the difference between the equilibrium concentration of O₂ and the steady-state concentration of O₂ in solution; in contrast, in a closed system (Fig. 7B), the respiration rate is proportional to the negative slope of the plot of O₂ concentration versus time. To stimulate respiration, glucose was added (Fig. 7C), whereupon the equilibrium concentration of O₂ fell. Respiration was followed at a constant stirring speed (and thus oxygen transfer rate) adjusted to give a near-steady-state around 50 % air saturation. When 100 μ M CORM-401 was added to the chamber (Fig. 7C), respiration clearly increased as evident in the further fall in dissolved O₂ concentration. This pattern resembles increases in respiration rates induced by substrate provision in *Klebsiella* (10). A similar increase in respiration rate was observed (28) when this concentration of CORM-401 was added to endothelial cells. The theory for O₂ transfer into a suspension culture is well known (for references see (10)): provided that the liquid-gas interface surface area is constant, the rate of O₂ transport from the gas to the liquid is given by $v = K_{La}(T_G - T_L)$, where v is the rate of respiration, K is a constant that depends on the experimental volume, surface area and temperature, T_G is the

Wareham: Antibacterial activities of a manganese CORM

molar concentration of O_2 in the liquid when equilibrated with air and T_L is the O_2 concentration in the liquid. In the non-proliferating cell suspensions used here, the slow decline in dissolved O_2 after a near-steady state was reached was neglected. We measured a K_{La} (11) of 0.23 min^{-1} (SD 0.06, 10 measurements) and a glucose-stimulated respiration rate of $215 \text{ nmol } O_2 \cdot \text{min}^{-1} \cdot \text{mg}^{-1}$ (SD 78, 13 measurements). In the experiment shown in Fig. 7C, respiration increased after adding $100 \mu\text{M}$ CORM-401 by 50%, typical of numerous experiments. This increase is similar to that observed before (28,52). As a control, 1 mM KCN (a potent respiratory inhibitor) was added to the chamber (Fig. 7C) when steady-state had been reached after adding CORM; dissolved oxygen then increased abruptly to pre-respiration levels indicating respiratory inhibition as expected. This pattern resembles decreases in respiration rate induced by substrate exhaustion in *Klebsiella* (10). The CORM 401-stimulated oxygen consumption can be assigned to cellular respiration, since it is cyanide-sensitive. The stimulation by CORM-401 was further investigated by using the same cell suspension (as Fig. 7C) but $10 \mu\text{M}$ carbonyl cyanide *m*-chlorophenyl hydrazone (CCCP), a classical uncoupler of respiration, was added to the chamber (Fig. 7C, inset). CCCP mimicked the effects of CORM-401; thus, both compounds stimulate oxygen consumption rates of *E. coli* cells.

In these experiments, dissolved oxygen was $>50\%$ saturation (approx. $100 \mu\text{M}$) at the point of adding CORM. However, maximal inhibition of respiration typically occurs at high $\text{CO}:O_2$ ratios since CO is a competitive inhibitor of terminal oxidases with oxygen; $\text{CO}:O_2$ ratios of 4:1 to 20:1 are used in photochemical action spectra (6). Thus, to maximize the potential inhibition of respiration by CORM-401, the stirring rotor speed was decreased to achieve a lower (but not zero) oxygen concentration in the chamber after stimulating respiration with glucose (Fig. 7D). On adding CORM-401, a very small, transient inhibition was seen. A second addition

of 100 μM CORM-401 (arrow 2) produced a mild but prolonged inhibition. To confirm these findings, 1 mM KCN was again added to the chamber and substantial inhibition followed. In the experiments of (28) 300 μM CORM-401 was required to inhibit respiration by endothelial cells. In summary, CORM-401 is not an effective inhibitor of respiration, even at low oxygen tensions, but stimulates respiration; such stimulation was described as ‘uncoupling’ in endothelial cells (28)

CORM-401, like CCCP, polarizes the membrane in whole cells

CCCP and other protonophores (‘uncouplers’) have dissociable protons and permeate membranes either as protonated acids or conjugated bases; they therefore facilitate proton exchange across energy-transducing membranes (43). To extend understanding of the energetic implications of CORM-401 administration, we measured membrane potential in whole cells using DiSC3(5) (61). DiSC3(5) is a cationic cyanine dye that responds fluorimetrically to changes in membrane potential by potential-dependent partition between the cells and the extracellular medium. When a cell or membrane interior becomes negatively charged (polarized), the dye is taken up with consequent fluorescence quenching (61). Depolarization on the other hand results in release of the dye and increase in fluorescence. The negatively-charged interior of respiring *E. coli* cells led to uptake of the dye and slow fluorescence quenching; to collapse the membrane potential ($\Delta\psi$) and depolarize the membrane, K^+ and the K^+ -specific ionophore valinomycin were added (Fig. 8A), whereupon net movement of the dye out of the cells resulted in increased fluorescence. However, a solution of CO (50 μM final concentration) did not significantly alter DiSC3(5) fluorescence (Fig. 8B). In marked contrast, addition of 50 μM CORM-401 (Fig. 8C) or only 1 μM CCCP (Fig. 8D) led to sustained decreases in

fluorescence over 15 min, demonstrating polarization of the membrane. Thus, both CORM-401 and CCCP stimulate respiration (Fig. 7) and increase polarization of the membrane (Fig. 8) (see Discussion). To determine whether membrane polarization was mediated by potassium flux across the membrane, the potassium gradient was first collapsed by valinomycin (Fig. 8E), followed by additions of CORM-401 (Fig. 8E) or valinomycin followed by CCCP (Fig. 8F). Addition of valinomycin caused a net movement of DiSC3(5) out of the cell, as in Fig. 8A, but when CORM-401 or CCCP was then added, polarization of the membrane was evident from the drop in fluorescence. In the case of CCCP, dramatic polarization was observed (an initial fluorescence decrease) as the collapse of the potassium charge gradient no longer impedes proton movement. The slower subsequent rise in fluorescence is attributed to a slow H^+ leak after initial hyperpolarization by CCCP. Therefore, the polarization caused by CORM-401 and CCCP is potassium-independent, suggesting involvement of H^+ or another cation.

Genes involved in potassium and general ion homeostasis and osmolarity are perturbed in response to CORM-401

In accord with the observed respiratory stimulation and membrane polarization elicited by CORM-401 (above), transcriptomic studies highlighted numerous genes involved in the transport of potassium and zinc, and genes involved in osmoregulation and ion homeostasis (Fig. 9). The KdpFABC complex is a multi-subunit ATP-driven potassium pump (24). All four genes encoding the membrane transporter were up-regulated within 5-10 min after CORM-401 treatment under aerobic conditions (Fig. 9). The *kdp* genes are expressed when K^+ levels in the cell become limited (33); this expression is regulated by KdpD (sensor kinase) and KdpE (response regulator) comprising a two-component regulatory system. However, measurements of

membrane polarization in the presence of valinomycin (Fig. 8) show that the CORM-401-elicited polarization is independent of potassium gradients, and so it is likely that the changes in *kdp* gene expression reflect global osmotic changes (30,34) and/or the physicochemical state of the membrane, as induced by ethanol, procaine and others (66). In addition to this high-affinity potassium transport system, *chaA*, encoding a $K^+/Na^+:H^+$ antiporter, was also transiently up-regulated both aerobically and anaerobically (Fig. 9). *E. coli* possesses two other K^+ transport systems, namely Kup and Trk, which exhibit a high transport velocity but low affinity and these are constitutively expressed, evidenced by the invariant levels of *trkA* expression (Fig. 9).

Two possible Ca^{2+} transporters have been identified in *E. coli*, including a Ca^{2+}/H^+ exchanger, ChaA, but it appears not to be a major Ca^{2+} -efflux pathway (42); the *chaA* gene was up-regulated by CORM-401 after 5 min both aerobically and anaerobically, further implicating osmotic imbalance (Fig. 9). ChaA has also been identified as a K^+/H^+ antiporter with roles in potassium homeostasis (54).

Other systems involved in osmoregulation were perturbed by CORM-401. Mechanosensitive channels are membrane transporters that respond to changes in cellular osmotic pressure (65). MscS is a homoheptameric, archetypal member of a diverse superfamily of mechanosensitive channels. It possesses a large water-filled cytoplasmic domain, and is involved in selectivity and may function as a “cytoplasmic osmometer” (47). In response to CORM-401, *mscS* was up to 5-fold up-regulated both aerobically and anaerobically (Fig. 9), suggesting osmotic stress, perhaps due to the uptake of the CORM.

We observed striking down-regulation (to undetectable levels; Supplementary Fig. S3 B) of the *ompF* gene encoding a large trimeric membrane permeability channel. The expression of this porin, and of the other major porin OmpC is exquisitely regulated (45). Because noxious

agents like antibiotics diffuse more readily through the larger OmpF channel, its increased production also facilitates entry of nutrients. Environmental osmotic status is sensed by the EnvZ component of the EnvZ-OmpR two-component system. High osmolarity activates OmpR, and *ompC* expression is increased and *ompF* expression decreases. The present data thus point to bacterial sensing of increased osmotic pressure. The OmpC and OmpF channels appear differentially regulated to tackle changes in osmotic pressure; OmpF may be down-regulated to avoid mass movement of unwanted solutes into the cell, including the CORM-401 compound itself, whilst expression of the smaller channel, OmpC, allows finer control of solute movement. Other systems that control turgor pressure include the aquaporin *aqpZ*, a water channel that allows the bidirectional movement of water in response to osmotic stress (62). This channel was slightly down-regulated in aerobic conditions in response to CORM-401 (Fig. 9).

Expression of a zinc-binding subunit of a zinc transporter (*znuA*) (51) was also up-regulated by 11-fold after 20 min aerobically (Fig. 9); anaerobically, a delayed rise peaked at 7-fold up-regulation after 40 min.

CORM-401 leads to changes in cellular potassium and zinc levels

Informed by the transcriptomic changes that indicated perturbation of metal ion homeostasis or osmolarity, and the demonstration that CORM-401 leads to membrane polarization, we measured potassium fluxes using spheroplast swelling experiments. Potassium movements with consequent swelling in the presence of CORMs have already been shown with CORM-3 (73), but CORM-401 did not induce spheroplast swelling in the presence of iso-osmotic potassium nitrate/potassium nitrite (data not shown). Although passive potassium movements appear not to be invoked by CORM-401, other data (above; up-regulation of *kdp* and

down-regulation of potassium efflux machinery) suggested that bacteria experienced potassium limitation. We therefore assessed the levels of total intracellular potassium and trace metals in the presence of CORM-401 using ICP-MS. Fig.10 shows that 67 μ M CORM-401 decreased the intracellular concentration of potassium and zinc by about 3-fold over 40 min. There were no measurable changes of copper or iron levels in response to CORM-401 addition, nor were genes implicated in the metabolism of these ions altered.

CORM-401 causes the induction of the Cpx and Bae regulons, altering the expression of Spy and CpxP protein but without measurable membrane damage to cells

The Cpx system in *E. coli* protects the membrane during stress (55), such as high osmolarity, leading to the management of cellular processes that include motility, chemotaxis (13) and biofilm formation (14). Exposure of cells to CORM-401 up-regulated numerous genes under the transcriptional control of Bae/Cpx (Fig. 11). Genes encoding the multidrug efflux system (*mdtA-D*) were more than 60-fold up-regulated under both aerobic and anaerobic conditions (Supplementary Fig. S3 C). Up-regulation of the Cpx response by CORM-2 (46) and involvement of the Cpx and Bae systems in response to CORM-3 have been noted previously (9,38). The most dramatic perturbation was that of the periplasmic chaperone Spy, which was up-regulated by >400-fold aerobically, and >600-fold anaerobically (Supplementary Fig. S3 C); CORM-3 elicits similar changes (9,38).

To determine whether the increased transcripts reflected protein levels, Western blot assays were carried out using antisera to two key players in the response, Spy and CpxP (74). Spy was detected in periplasmic fractions of wild type cells and CpxP was measured in total soluble (cytoplasmic and periplasmic) fractions. Addition of 67 μ M CORM-401 significantly

Wareham: Antibacterial activities of a manganese CORM

increased Spy protein levels after 2 h (Fig. 12B, lane 3), whereas incubation with the control compounds MnSO₄ and DTC did not raise Spy to detectable levels (Fig. 12B, lane 2); the control in the absence of CORM showed no detectable Spy (Fig. 12B, lane 1). Levels of the periplasmic chaperone CpxP were clearly detected in the absence of CORM (Fig. 12B, lane 1) and also on incubation with control compounds (Fig. 12B, lane 2), but a significant decrease in CpxP abundance was seen after 2 h CORM-401 treatment (lane 3). The CORM-induced decrease in CpxP is consistent with literature on the Cpx response (55); since CpxP is a negative regulator its levels are lowered to achieve the Cpx response evident in Fig. 11.

CORM-3 up-regulates *spy* expression and increases Spy levels due to membrane damage (74). The effects of CORM-401 on bacterial outer membranes was therefore assayed using *N*-phenyl-1-naphthylamine (NPN), a membrane-impermeable fluorophore that increases fluorescence in a hydrophobic environment (61). Thus, when the bacterial membrane becomes perturbed (e.g. by an antibiotic or CORM-401), the dye partitions into the outer-membrane leading to an increase in fluorescence. Interestingly, the addition of CORM-401 to cells in the presence of NPN showed no increase in membrane damage, even after several hours (Fig. 12C). The detergent Triton X-100 was used as a positive control (Fig. 12C). Thus the action of CORM-401 is distinct from CORM-3: the up-regulation of Spy protein and transcript levels by CORM-401 appears indirect and due to perturbation of cellular osmotic balance and metal ion homeostasis.

The *spy* gene is positively regulated by phosphorylated CpxR whereas several motility genes are negatively controlled (13). Indeed, Fig. 4 shows that on incubating bacteria with CORM-401 for 5 or more min, the expression of motility genes was decreased. However, within the first 5 min of exposure to CORM-401 or after 80 min incubation, a majority of motility genes

was up-regulated (Fig. 2). To resolve this, we measured motility (swarming) as before (38). After 48 h incubation, the mean colony diameters were measured as 12.2 (\pm 2.2 SD) mm for control colonies whereas cells grown with 67 μ M CORM-401 (as used for Fig. 4) had an increased colony diameter of 24.2 (\pm 0.8 SD) mm (data not shown). However, control compounds Mn(II) sulfate and sarcosine DTC increased motility further (colony diameter of 32.3 \pm 2.3 SD mm). The Student's t-test revealed that the difference between these data sets was highly significant (p-value < 0.001). We conclude that bacterial motility is not modulated by intact CORM-401.

A CORM-401 growth screen of several pathogens isolated from clinical infections show varying susceptibility

To broaden the significance of this study, eight clinical isolates of pathogenic bacteria were tested for their sensitivity to the title compound. *E. coli* EC958 is a multi-drug resistant O25b:H4 clinical pathogen (68). The genome encodes numerous putative virulence factors including siderophore receptors, auto-transporters and bears genes conferring resistance to ciprofloxacin and other antibiotics (68). We also tested clinical isolates of *Klebsiella pneumoniae*, *Shigella flexneri*, *Pseudomonas aeruginosa*, *Salmonella enterica* serovar Kedougou, *Enterobacter hormaechei*, *Citrobacter koseri* and *Acinetobacter baumannii*. Cultures were grown to early-exponential phase prior to the addition of CORM-401 (final concentration, 500 μ M). Growth was monitored until stationary phase was reached in cultures not exposed to the compound (Fig. 13). Addition of the metal carbonyl caused a complete arrest in growth for *K. pneumoniae*, *E. coli* EC958, *S. flexneri*, *S. Kedougou* and *E. hormaechei* cultures; however growth of *P. aeruginosa*, *C. koseri* and *A. baumannii* was unperturbed by the compound.

CORM-401 toxicity in combination with antibiotics

A promising approach to the rise of antibiotic-resistant bacteria, compounded by slow emergence of new drugs, is the use of non-antibiotic compounds to complement existing antibiotics (15,20). While antibiotics generally target specific cellular processes, such as DNA replication, and synthesis of cell walls and proteins, CORMs have numerous targets, as evidenced here. Thus we tested CORM-401 interactions with two antibiotics, cefotaxime and trimethoprim, against strain MG1655. Addition of 100 μ M CORM-401 with antibiotics at sub-lethal doses, led to a greater, statistically significant, reduction of growth compared to either the antibiotic or CORM-401 alone (Figs. S4 A, B). However, viability assays with cefotaxime (Fig. S4 C) or trimethoprim (Fig. S4 D) showed that each antibiotic and CORM-401 significantly reduced viable cell numbers, even when used individually. To quantify these interactions, we used checkerboard dilution plates and calculated the fractional inhibitory concentrations (FIC) for each combination. For cefotaxime and trimethoprim (Fig. S4) as well as for novobiocin and cefotaxime, FIC values were between 0.54 and 0.91 (Table 1), indicative of no interaction (48) between the two antimicrobial compounds.

The World Health Organization, in its recent global priority list of antibiotic-resistant bacteria, identifies antibiotic-resistant Enterobacteriaceae, including *E. coli*, as being amongst the most critical (71). Because of the broad antibiotic resistance of strain EC958, we selected colistin (a 'drug of last resort'), doxycycline and gentamycin. In each case, FIC values were between 0.56 and 1.03 (Table 1), again indicative of no interaction between the two antimicrobial compounds. In conclusion, the bactericidal and bacteriostatic activities of CORM-401 are not synergistic with antibiotic action.

Discussion

CORMs, originally devised to mimic the beneficial antioxidant, anti-inflammatory and cytoprotective benefits of CO, serendipitously proved to be effective antimicrobial agents. In particular, the ruthenium compounds CORM-2 and CORM-3 are highly effective antimicrobials (12,73), but the basis of their efficacy remains unresolved. CO release appears to be a minor contributor to microbial toxicity and attention has turned to the role of Ru (63).

Interestingly, a manganese photoactivated CORM, $[\text{Mn}(\text{CO})_3(\text{tpa-}\kappa^3\text{N})]^+$, is less effective than the Ru complexes (41), unless combined with hydrogen peroxide (67). The present compound, CORM-401 is also a manganese complex, on which few studies are published. In previous work, it released 2.1-3 mol CO in the myoglobin assay (16), in line with our determination of 2.4-2.5 mol in minimal growth medium or phosphate buffer and with myoglobin at a 4-fold excess over CORM-401. In mammalian studies, the higher CO yield elicited more effective aortic relaxation and vasodilation than did CORM-A1, which has a similar half-time of CO release but a lower molar CO yield. CORM-401 reduces inflammation and damage in pig kidneys in a pre-clinical model of organ donation (3) and reverses the metabolic changes that occur during lipopolysaccharide-induced microglia inflammation (72).

In endothelial cells, there is evidence that the CO released from CORM-401 uncouples mitochondrial respiration and inhibits glycolysis (28), since 'inactive CORM-401 (iCORM)' (actually a mix of MnSO_4 and the CORM-401 ligand DTC) did not induce these effects. However, even 300 μM CORM-401 elicited only a c. 2-fold elevation in oxygen consumption rate, whereas only 1 μM CCCP gave greater stimulation (28). CORM-401 therefore exerts relatively weak but clear uncoupler-like activity in mammalian cells, a result confirmed here in

bacteria (Fig. 7C). In endothelial cells, CORM-401 also reactivated mitoBK_{Ca} channels after blockage with paxilline (28). The mechanistic basis of most of these effects on mitochondria is unclear, but it is assumed that, at the highest CORM concentrations, the decrease in respiration rate is due to inhibition of cytochrome oxidase activity (28). Activation of mitochondrial uncoupling proteins has been proposed to explain CORM-3-uncoupled metabolism in cardiomyocytes (36).

Our data suggest an alternative mode of action for growth inhibition of *E. coli* (Fig. 1) and many other bacteria (Fig. 14) and the myriad effects of CORM-401. First, the released CO does target terminal oxidases (Fig. 7A) leading to slight reductions in oxygen consumption rates (Fig. 7B, D), but the stimulatory effects on respiration are much more significant (Fig. 7C). In-depth transcriptomic and modelling studies (Fig. 4 – 6) confirm effects on respiratory gene regulation. More striking are the elevations in intracellular Mn concentrations (and thus the CORM, Fig. 3). We suggest that buildup of the metal co-ligand fragment in the cytoplasm to millimolar concentrations leads to disruption of charge (Fig. 8) and ion balance (Fig. 10) and the ‘perception’ by the cell that it is undergoing osmotic stress (Fig. 9, 11, 12). These ideas are summarised in Fig. 14. The mechanism of polarization caused by CORM-401 is unclear but is independent of potassium gradients (Fig. 8) and presumably caused by perturbation of other ionic balances across the membrane. In mammalian systems also, the CORM-401-enhanced resistance of cardiomyocytes to oxidative stress may be at least in part due to the manganese center (31). However, in contrast to (28), we cannot attribute the effects on membrane polarization to the released CO, since a CO gas solution is without effect on membrane potential (Fig. 8B). Our proposals that CORM-401 toxicity are not dependent on respiratory inhibition are

1
2
3 in accord with other studies, notably, the finding that CORM-3 is toxic to bacteria even in the
4
5 absence of a heme target (74).
6
7

8 CORM-401 stimulates mitochondrial (28) and bacterial ((73); this work) respiration, a
9
10 response mimicked by the classical uncoupler CCCP (Fig. 7C). However, the fact that CORM-
11
12 401, like CCCP, caused polarization of the membrane (Fig. 8) suggests that this is compensated
13
14 by enhanced respiration. That bacteria remain viable after CCCP treatment and can mount such a
15
16 respiratory response is evidenced by the fact that neither 100 μ M CORM-401 (this work, Fig. 2)
17
18 nor 1 μ M CCCP significantly inhibit growth and respiration remains responsive to imposed
19
20 membrane conditions. Indeed, 1 μ M CCCP elicits only a 2% decrease in swimming speed of *E.*
21
22 *coli* (4).
23
24
25
26

27 CORM-401 has a net negative charge in solution, yet is rapidly accumulated to
28
29 millimolar levels in the cell (Fig. 3A). The charged metal species produced when the compound
30
31 releases CO might also affect charge separation across the membrane. It is expected that when
32
33 CO groups are released from CORM-401, the metal in the residual co-ligand fragment will
34
35 become oxidized giving a Mn(II) species. It is therefore interesting that, upon CORM-401
36
37 addition, cells become polarized; this may be due to perturbation of charge separation across the
38
39 membrane or by the accumulation of “compatible solutes”, with little or no negative charge, to
40
41 balance the influx of positive charge (75). In addition to polarization, loss of K^+ and Zn(II) from
42
43 the cell (Fig. 10) may result from accumulation of charge. The mechanosensitive channel MscS,
44
45 which is up-regulated in response to osmotic pressure, was also up-regulated (Fig. 9). We
46
47 suggest that a contributing factor to the action of CORM-401 is generation of a high osmotic
48
49 pressure upon extreme accumulation of the compound (Fig. 3). Although cellular envelope stress
50
51 responses are up-regulated at the transcriptomic and protein levels, and transport systems for
52
53
54
55
56
57
58
59
60

metal ions and water are differentially expressed in response to CORM-401 (Fig. 8), CORM-401, unlike CORM-3, has little effect on the cell membrane as assessed by NPN fluorescence.

Here we demonstrate for the first time that CORM-401 also has broad-spectrum antimicrobial activities. However, CORM-401 exhibits toxicity towards eukaryotic cells: at 100 μM , a 25% decrease in viability of RAW264.7 cells was noted (7), whereas this concentration had little effect on *E. coli* viability up to 4 h (Fig. 2 C, D). CORM-401 toxicity is dependent on the carbon source used in the growth of the bacterium, probably reflecting differences in uptake (Fig. 3). Although CO released from CORM-3 and $([\text{Mn}(\text{CO})_3(\text{tpa}-\kappa^3\text{N})]^+)$ binds cellular targets such as the respiratory heme oxidases, recent data suggest that CORMs display numerous other modes of toxicity.

The multiple modes of action of CORM-401 and other CORMs are clearly distinct from the focused effects of most antibiotics, suggesting that these compounds, even before we comprehensively understand their targets, should be valuable as antimicrobial agents that could enhance antibiotic sensitivities. Indeed, CORM-401 enhances, without interaction, the efficacy of four antibiotics on *E. coli* (Table 1). It is notable that CO gas neither potentiates the toxicity of antibiotics nor protects from their effects (69).

The different sensitivities of clinical isolates to CORM-401 probably reflect different metabolism and import/export mechanisms. The resistance of *P. aeruginosa* to CORM-401 appears contrary to the results of previous research using CORM-2 (40). However, *P. aeruginosa* and *A. baumannii* express multiple efflux pumps, making them resistant to numerous antibiotics (19,64). The hypothesis that these strains fail to accumulate CORM-401 intracellularly might be tested by analyses of manganese contents and comparison of sensitive and resistant strains.

Resistance to CORM-401 may also reflect the ability of resistant bacteria to produce and excrete

1
2
3 mucoid substances forming a peripheral capsule around the pathogens, hindering access of the
4
5 metal carbonyl compound. Capsule production decreases sensitivity to antibiotics and renders
6
7 pathogens resistant to phagocytosis by macrophages and to the toxic effects of free radical
8
9 species (21,22). The potential for CORMs to act as novel antimicrobials against other clinical
10
11 isolates is indicated by the sensitivity of numerous bacterial species, including several members
12
13 of the family Enterobacteriaceae. For example, the sensitivity of the urinary tract and
14
15 bloodstream pathogen *E. coli* EC958 to CORM-401 suggests that exploration of these CO-
16
17 releasers as potential anti-UTI drugs either alone or with current antibiotics is a realistic
18
19 possibility.
20
21
22
23
24

25 An ongoing challenge is to understand the bases of the antimicrobial actions of CORMs
26
27 and use this knowledge to devise scaffolds with increased activity. Although CORM-401 is a
28
29 less effective antimicrobial agent than CORMs-2 or -3, such data contribute to our understanding
30
31 of the effects of CORMs in general and the development of future CORMs as antimicrobials;
32
33 greater consideration of the effect of the metal center could lead to the generation of more potent
34
35 and biologically-compatible CORMs.
36
37
38
39
40
41
42
43
44
45
46
47
48
49
50
51
52
53
54
55
56
57
58
59
60

Innovation

It is essential to investigate new CORMs if the promised prospects of site-specific and time-controlled release of CO are to be exploited. We report the first detailed microbiological characterization of the toxicity of the water-soluble CORM-401, $[\text{Mn}(\text{CO})_4(\text{S}_2\text{CNMe}(\text{CH}_2\text{CO}_2\text{H}))]$, to *E. coli* strains and other pathogens. Our findings that CORM-401 is an ineffective inhibitor of growth and respiration (despite being accumulated to high levels), yet exerts profound effects on the bacterial membrane and global gene expression cast doubt on the mechanism of action of this CORM and others. Such insights open the way for new compound design and novel clinical, combinatorial therapies.

(100 words)

Materials and Methods

E. coli strains and batch growth conditions

E. coli K12 derivative MG1655 was used as a model organism for this study; other pathogenic clinical isolates were tested where indicated. All strains were grown in Evans medium with glucose or succinate (20 mM each) as the carbon source (27). For *S. flexneri* and *A. baumannii* MEM Amino Acids (50x – Sigma-Aldrich) solution was added to facilitate growth. Unless stated, cells were grown to mid-exponential phase ($OD_{600} \sim 0.5-0.6$, 50-60 Klett units) before adding CORM-401 or other compounds. Growth was monitored using a Klett-Summerson colorimeter using a red filter in 250 ml conical flasks fitted with side arms or spectrophotometrically at 600 nm. Note that bacterial cultures begin growth at different intervals after inoculation so that averaging several similar experiments on a time basis is inappropriate. Growth curves generally show one experiment representative of 3 or more that showed similar kinetics and growth rates.

Chemostat growth conditions

For continuous culture, cells were grown in an Infors Multifors bioreactor (total volume 200 ml) adapted to fit a Labfors-3 fermenter base unit. Temperature was maintained at 37 °C with continuous stirring at 200 rpm; the dilution rate was 0.2 h^{-1} . Mass flow controllers allowed gas mixes for aerobic and anaerobic conditions to be maintained by continuous bubbling at 100 ml min^{-1} with air and N_2 gas (aerobic) or N_2 gas alone (anaerobic) as before (38).

CORM-401 and control compounds

Wareham: Antibacterial activities of a manganese CORM

CORM-401 was synthesized in the Department of Chemistry, The University of Sheffield as before (7). Stock solutions (5 mM) were prepared fresh daily in phosphate-buffered saline (PBS), pH 7.4. There is no useful 'iCORM', i.e. an inactive compound for control experiments; instead, MnSO_4 (0.1 M stock solution) and sodium dithiocarbamate (DTC, $\text{Na}[\text{S}_2\text{CN}(\text{CH}_3)\text{CH}_2\text{COONa}]$, 10 mM stock solution) were combined to give equimolar mixes of the two compounds, as required. Once the Mn in CORM-401 loses CO, the Mn(I) will probably be oxidised to Mn(II). Mn(II) is kinetically labile and it is probable that the $[\text{O}_2\text{CCH}_2\text{NMeCS}_2]^{2-}$ ligand dissociates. Others refer to such a mixture as 'inactive CORM-401' (16) but its physiological and transcriptomic effects have not been evaluated.

Myoglobin assay for CO release

CO liberated from CORM-401 was assayed using the reaction with ferrous myoglobin (39) but final concentrations of myoglobin and CORM were 15 μM and 3 μM , respectively (to allow equistoichiometric binding to myoglobin of the anticipated 3-4 mol CO released from CORM-401). All assays were carried out at 37 °C unless otherwise indicated.

Subcellular fractionation and metal analyses

Exponential cultures (1 l) were supplemented with 67 μM CORM-401 or, as a control, DTC/ MnSO_4 and incubated at 37 °C with shaking at 200 rpm for 90 min before centrifugation (10 min, 12 000 x g). The supernatant was retained for analysis and the cell pellet was resuspended in ~ 6 ml of 200 mM PBS (pH 7.0) before sonication on ice (MSE Soniprep, 16 μm , 6 x 15 s bursts). Following centrifugation (20 min, 20 000 x g) the pellet comprising cell debris was discarded. From the supernatant, membrane and cytoplasmic fractions were isolated by

ultracentrifugation (60 min, 160 000 x g) using centrifuge tubes pre-washed in concentrated nitric acid to remove trace metals. Samples of genomic DNA were isolated from independently grown cultures under identical growth conditions using the Wizard[®] Genomic DNA Purification Kit and the manufacturer's instructions. Metals were assayed in all fractions by inductively coupled plasma-mass spectrometry, as described below.

Assay of CO binding to cellular heme proteins

Spectra were recorded with an Olis RSM1000 dual-beam rapid scanning monochromator (On-Line Instrument Systems) fitted with a CLARiTY accessory as before (56). Cells were resuspended in PBS to an OD ~ 55 and CORM-401 was added to a final concentration of 100 μ M. Scans were taken at intervals up to 15 min after addition of CORM-401.

Assays of cellular respiration

In closed-electrode experiments, oxygen consumption was measured using a Clark-type electrode (27) (Rank Brothers, Bottisham, Cambridge, UK). The chamber contents (2 ml) were stirred at 37 °C while the top was sealed with a close-fitting lid that permitted addition via microsyringes of reagents. For prolonged measurements of respiration, a custom electrode apparatus open to the atmosphere, based on published designs (11) was used. The Perspex cell (working volume 4 ml) was maintained at 37 °C by circulating water, the cell being constructed of stainless steel to aid temperature equilibration. The two-bladed stirring impeller (diameter 14 mm) was mounted on a stainless steel shaft that was stirred using an overhead stirrer (IKA[®]-Werke Eurostar power control-visc P4) to maintain a stable vortex and absolute constancy of rotational speed, and therefore of transfer of air from the atmosphere to the stirred sample. The

rate of oxygen diffusion from the atmosphere to the sample was expressed as K_La , measured as in (52). The additions made were of CORM-401 (stock solution 5 mM), carbonyl cyanide *m*-chlorophenylhydrazone (CCCP; stock solution 10 mM), or KCN (stock solution 15 mM).

Assays of membrane potential

Cells were washed, resuspended in 5 mM HEPES buffer to a final OD₆₀₀ of 0.6 and incubated with 0.1 M KCl and 10 mM glucose before treatment for ~ 5-10 min with 0.4 μ M DiSC3(5) in a 3 ml quartz cuvette. Fluorescence was measured as before using a Hitachi F-2500 fluorescence spectrophotometer.

Assays of cell motility

Motility assays were performed as previously described (38). Briefly, *E. coli* MG1655 cells were aerobically grown to stationary phase in glucose-supplemented Evans medium and 10 μ l of the liquid culture was spotted onto 0.3% (w/v) LB/agar plates containing 67 μ M CORM-401 or the control compounds DTC/MnSO₄. Plates were incubated for 48 h at 30 °C and colony diameters measured. Each of 3 biological replicates comprised 5 technical determinations.

Transcriptomic analysis and statistical modelling

These procedures were conducted as before (38,69,74) except that samples were taken from chemostat cultures of glucose-grown cells immediately prior to CORM-401 addition and at intervals thereafter. In brief, extracted RNA was labeled with Cy-3 or Cy-5-dCTP, and hybridized to Agilent arrays that were scanned using an Agilent DNA SureScan Microarray scanner with subsequent feature extraction and data analysis using GeneSpring GX v7.3.

Arbitrary values of ≥ 2 -fold (i.e. ≥ 2 -fold increased expression) or ≤ 0.5 -fold (i.e. ≤ 2 -fold decreased expression) were chosen to identify genes with significantly altered expression. Functional category gene lists were created using KEGG (Kyoto Encyclopedia of Genes and Genomes) (69). Where available, regulatory proteins for each gene were identified using EcoCyc (<https://ecocyc.org/>). Modelling of transcription factor activities using TFInfer (2,23,58), and measuring similarity in transcription factor activities between two different conditions, were performed as described in (38).

Metal analyses

Culture samples (20 ml) samples were taken before and after addition of 67 μM or 500 μM CORM-401 and assayed for metal content as before (38). Intracellular metal concentrations were calculated using literature values for cell volume (23). In control experiments, cultures were treated instead with 500 μM MnSO_4 +/- 67 μM DTC, or a saturated solution of CO giving 500 μM CO final concentration. To estimate total numbers of manganese atoms per cell, the data of Outten and O'Halloran (49) were used.

Outer membrane permeabilization assays

Outer membrane (OM) permeability of CORM-401 was assayed using 1-N-phenylnaphthylamine (NPN) (61) at a final concentration of 1 μM . Cells were grown to exponential phase (OD_{600} of 0.6), pelleted, then washed and re-suspended in PBS. The final cell suspension was adjusted to an OD_{600} of ~ 0.5 . Fluorescence was measured ($\lambda_{\text{ex}} = 340 \text{ nm}$, $\lambda_{\text{em}} = 420 \text{ nm}$) using a Hitachi F-2500 fluorescence spectrophotometer.

Spheroplasts and osmotic swelling measurements

To measure transmembrane ion fluxes, osmotic swelling was measured by following changes in turbidity at 500 nm following dilution of spheroplasts in iso-osmotic (0.25 M) salt solutions as before except that EDTA/lysozyme treatment was at 37 °C (74).

Western blotting for Spy and CpxP detection

This was done as before (74). In brief, CORM-401 or DTC/MnSO₄ were added to cultures to a final concentration of 67 µM and incubated for 2 h. For Spy quantitation, periplasmic fractions were isolated using the Tris/sucrose/EDTA (TSE) method (53). For CpxP, soluble fractions were made after cell breakage by sonication, differential centrifugation, followed by reduction with 200 mM dithiothreitol and separation by SDS-PAGE. Proteins were blotted using primary rabbit anti-Spy/CpxP antibodies at 1:25,000/1:50,000 dilutions, respectively. Anti-rabbit secondary antibodies were incubated at a concentration of 1:50,000 before detection using the ECL-Plus Western system (Amersham).

Growth and viability studies of CORM-401 in conjunction with antibiotics

Bacteria were grown in Evans medium with 20 mM glucose as a carbon source until 0.3 OD₆₀₀ was reached; CORM-401 (100 µM) and/or trimethoprim (1.0 µg/ml) or cefotaxime (1.0 µg/ml) were added alone or in combination. The interactions of CORM-401 with antibiotics were determined using a broth micro-dilution checkerboard assay (44). Briefly, bacteria were diluted in Evans medium to reach an OD around 0.3 (approx. 5x10⁵ cfu/ml) and 200 µl of the suspension pipetted into each well of a 96 well plate. The concentrations used for wild-type MG1655 were: CORM-401 (100 – 600 µM), trimethoprim (1 – 16 µg/ml) and cefotaxime (1.0 –

32 µg/ml). For strain EC958 concentrations were: CORM-401 (37.5 – 600 µM), colistin (0.25 – 8 µg/ml), doxycycline (6 – 96 µg/ml) and gentamicin (0.125 – 4 µg/ml) added alone or in combination with CORM-401. Cultures were incubated at 37 °C with shaking for 24 h using a Tecan Sunrise plate reader. The concentrations tested were up to four 2-fold dilutions lower than the MIC and, where possible, two 2-fold dilutions higher than the MIC. The minimal inhibitory concentration (MIC) was considered as the lowest concentration of the agent alone, or combined with CORM-401, that inhibited growth. Fractional inhibitory concentration index (FICI) (44) was calculated to determine drug interaction, and interpreted as follows: FICI of two-drug combination = $FIC_A + FIC_B$, where FIC_A is the MIC of drug A in combination with CORM-401/MIC of drug A alone and FIC_B is the MIC of drug B in the combination with CORM-401/MIC of drug B alone. The results indicate synergy when the calculated $FICI \leq 0.5$, no interaction when $FICI > 0.5-4$, and antagonism when the $FICI > 4$ (48).

Statistical Analysis

All data are expressed as the mean ± SEM, unless otherwise stated. The comparison of the means was performed using Student’s *t*-test for two groups of data. For comparison of data across more than two groups, ANOVA followed by Bonferroni’s multiple comparison tests were used. When $P < 0.05$, data were considered significantly different.

Acknowledgements

We are especially grateful to our selected open peer reviewers (see comments in *Supplementary Text* online) as well as Simon Avery, Emanuel Buys, Tom Coenye, Greg Cook, David Lloyd, William Navarre, Frank Sargent and Gary Sawers, who gave their time generously in reviewing

Wareham: Antibacterial activities of a manganese CORM

this work. Thomas W Smith provided helpful discussions on the chemistry of CORMs. This work was supported by the Biotechnology and Biological Sciences Research Council (UK, BBSRC), The Leverhulme Trust, and the Kurdistan Regional Government (KRG, Iraq). G.S. acknowledges support from the European Research Council under grant MLCS306999.

Author Disclosure Statement

No competing financial interests exist.

Abbreviations Used

CCCP = carbonylcyanide *m*-chlorophenylhydrazone

DTC = dithiocarbamate, Na[S₂CN(CH₃)CH₂COONa]

FICI = fractional inhibitory concentration index

ICP-MS = inductively coupled plasma mass spectrometry

OM = outer membrane

PBS = phosphate-buffered saline

PTS = phosphotransferase system

References

1. Alvarez AF and Georgellis D. In vitro and in vivo analysis of the ArcB/A redox signaling pathway. *Methods in Enzymology, Vol 471: Two-Component Signaling Systems, Part C* 471: 205-228, 2010.
2. Asif HM, Rolfe MD, Green J, Lawrence ND, Rattray M and Sanguinetti G. TFInfer: a tool for probabilistic inference of transcription factor activities. *Bioinformatics* 26: 2635-6, 2010.
3. Bhattacharjee R, Mohamed MR, Saha M, Solis KP, Mayer R, Barrett P, AlHasan I, Aboalsamh G, Cepinskas G and Luke P. Warm perfusion of carbon monoxide releasing molecule 401 reduces inflammation and damage in preclinical donation after cardiac death kidney transplantation model. *J Urol* 195: E430-E430, 2016.
4. Bogachev AV, Murtazina RA, Shestopalov AI and Skulachev VP. Induction of the *Escherichia coli* cytochrome *d* by low $\Delta\mu_{\text{H}^+}$ and by sodium ions. *Eur J Biochem* 232: 304-308, 1995.
5. Bongaerts J, Zoske S, Weidner U and Unden G. Transcriptional regulation of the proton translocating NADH dehydrogenase genes (*nuoA-N*) of *Escherichia coli* by electron acceptors, electron donors and gene regulators. *Mol Microbiol* 16: 521-534, 1995.
6. Castor LN and Chance B. Photochemical action spectra of carbon monoxide-inhibited respiration. *J Biol Chem* 217: 453-465, 1955.
7. Crook SH, Mann BE, Meijer A, Adams H, Sawle P, Scapens D and Motterlini R. $\text{Mn}(\text{CO})_4\{\text{S}_2\text{CNMe}(\text{CH}_2\text{CO}_2\text{H})\}$, a new water-soluble CO-releasing molecule. *Dalton Trans* 40: 4230-4235, 2011.
8. Davidge KS, Motterlini R, Mann BE, Wilson JL and Poole RK. Carbon monoxide in biology and microbiology: surprising roles for the "Detroit perfume". *Adv Microb Physiol* 56: 85-167, 2009.
9. Davidge KS, Sanguinetti G, Yee CH, Cox AG, McLeod CW, Monk CE, Mann BE, Motterlini R and Poole RK. Carbon monoxide-releasing antibacterial molecules target respiration and global transcriptional regulators. *J Biol Chem* 284: 4516-4524, 2009.
10. Degn H, Lilleor M and Iversen JLL. The occurrence of a stepwise-decreasing respiration rate during oxidative assimilation of different substrates by resting *Klebsiella aerogenes* in a system open to oxygen. *Biochem J* 136: 1097-1104, 1973.
11. Degn H, Lundsgaard JS, Petersen LC and Ormicki A. Polarographic measurement of steady state kinetics of oxygen uptake by biochemical samples. *Meth Biochem Anal* 26: 47-77, 2006.
12. Desmard M, Davidge KS, Bouvet O, Morin D, Roux D, Foresti R, Ricard JD, Denamur E, Poole RK, Montravers P, Motterlini R and Boczkowski J. A carbon monoxide-releasing molecule (CORM-3) exerts bactericidal activity against *Pseudomonas*

- aeruginosa* and improves survival in an animal model of bacteraemia. *FASEB J* 23: 1023-1031, 2009.
13. DeWulf P, Kwon O and Lin ECC. The CpxRA signal transduction system of *Escherichia coli*: Growth-related autoactivation and control of unanticipated target operons. *J Bacteriol* 181: 6772-6778, 1999.
 14. Dorel C, Vidal O, Prigent-Combaret C, Vallet I and Lejeune P. Involvement of the Cpx signal transduction pathway of *E. coli* in biofilm formation. *FEMS Microbiol Lett* 178: 169-75, 1999.
 15. Ejim L, Farha MA, Falconer SB, Wildenhain J, Coombes BK, Tyers M, Brown ED and Wright GD. Combinations of antibiotics and nonantibiotic drugs enhance antimicrobial efficacy. *Nat Chem Biol* 7: 348-50, 2011.
 16. Fayad-Kobeissi S, Ratovonantenaina J, Dabire H, Wilson JL, Rodriguez AM, Berdeaux A, Dubois-Rande JL, Mann BE, Motterlini R and Foresti R. Vascular and angiogenic activities of CORM-401, an oxidant-sensitive CO-releasing molecule. *Biochem Pharmacol* 102: 64-77, 2016.
 17. Fewson CA, Poole RK and Thurston CF. Spectrophotometry in microbiology: symbols and terminology, scattered thoughts on opaque problems. *Soc Gen Microbiol Q* 11: 87-89, 1984.
 18. Fukuto JM, Carrington SJ, Tantillo DJ, Harrison JG, Ignarro LJ, Freeman BA, Chen A and Wink DA. Small molecule signaling agents: the integrated chemistry and biochemistry of nitrogen oxides, oxides of carbon, dioxygen, hydrogen sulfide, and their derived species. *Chem Res Toxicol* 25: 769-93, 2012.
 19. Giamarellou H, Antoniadou A and Kanellakopoulou K. *Acinetobacter baumannii*: a universal threat to public health? *Int J Antimicrob Agents* 32: 106-19, 2008.
 20. Gill EE, Franco OL and Hancock RE. Antibiotic adjuvants: diverse strategies for controlling drug-resistant pathogens. *Chem Biol Drug Des* 85: 56-78, 2015.
 21. Govan JR and Deretic V. Microbial pathogenesis in cystic fibrosis: mucoid *Pseudomonas aeruginosa* and *Burkholderia cepacia*. *Microbiol Rev* 60: 539-74, 1996.
 22. Govan JR and Fyfe JA. Mucoid *Pseudomonas aeruginosa* and cystic fibrosis: resistance of the mucoid from to carbenicillin, flucloxacillin and tobramycin and the isolation of mucoid variants *in vitro*. *J Antimicrob Chemother* 4: 233-40, 1978.
 23. Graham AI, Sanguinetti G, Bramall N, McLeod CW and Poole RK. Dynamics of a starvation-to-surfeit shift: a transcriptomic and modelling analysis of the bacterial response to zinc reveals transient behaviour of the Fur and SoxS regulators. *Microbiology-Sgm* 158: 284-292, 2012.
 24. Greie JC. The KdpFABC complex from *Escherichia coli*: a chimeric K⁺ transporter merging ion pumps with ion channels. *Eur J Cell Biol* 90: 705-10, 2011.
 25. Iuchi S, Chepuri V, Fu HA, Gennis RB and Lin ECC. Requirement for terminal cytochromes in generation of the aerobic signal for the *arc* regulatory system in

Wareham: Antibacterial activities of a manganese CORM

- Escherichia coli*: study utilizing deletions and *lac* fusions of *cyo* and *cyd*. *J Bacteriol* 172: 6020-6025, 1990.
26. Iuchi S and Lin ECC. Adaptation of *Escherichia coli* to redox environments by gene expression. *Mol Microbiol* 9: 9-15, 1993.
 27. Jesse HE, Nye TL, McLean S, Green J, Mann BE and Poole RK. The terminal oxidase cytochrome *bd-I* in *Escherichia coli* has lower susceptibility than cytochromes *bd-II* or *bo'* to inhibition by the carbon monoxide-releasing molecule, CORM-3: N-acetylcysteine reduces CO-RM uptake and inhibition of respiration. *Biochim Biophys Acta* 1834: 1693-1703, 2013.
 28. Kaczara P, Motterlini R, Rosen GM, Augustynek B, Bednarczyk P, Szewczyk A, Foresti R and Chlopicki S. Carbon monoxide released by CORM-401 uncouples mitochondrial respiration and inhibits glycolysis in endothelial cells: A role for mitoBK(Ca) channels. *Biochim Biophys Acta-Bioenergetics* 1847: 1297-1309, 2015.
 29. Keilin D. *The History of Cell Respiration and Cytochrome* Cambridge: Cambridge University Press; 1966. 416 p.
 30. Kempf B and Bremer E. Uptake and synthesis of compatible solutes as microbial stress responses to high-osmolality environments. *Arch Microbiol* 170: 319-30, 1998.
 31. Kobeissi SF, Wilson JL, Michel B, Dubois-Rande J-L, Motterlini R and Foresti R. Pharmacological activities of CORM-401, a redox-sensitive carbon monoxide-releasing molecule, in H9C2 cardiomyocytes. *Archiv Cardiovasc Dis Suppl* 6, 2014.
 32. Koch AL. Growth measurement. In: *Methods for General and Molecular Bacteriology*. edited by Gerhardt P, Murray RGE, Wood WA, Krieg NR. Washington, D.C.: American Society for Microbiology; 1994. pp. 248-277.
 33. Laermann V, Cudic E, Kipschull K, Zimmann P and Altendorf K. The sensor kinase KdpD of *Escherichia coli* senses external K⁺. *Mol Microbiol* 88: 1194-204, 2013.
 34. Laimins LA, Rhoads DB and Epstein W. Osmotic control of *kdp* operon expression in *Escherichia coli*. *Proc Natl Acad Sci U S A* 78: 464-8, 1981.
 35. Leffler CW, Parfenova H and Jaggar JH. Carbon monoxide as an endogenous vascular modulator. *Am J Physiol Heart & Circ Physiol* 301: H1-H11, 2011.
 36. Lo Iacono L, Boczkowski J, Zini R, Salouage I, Berdaux A, Motterlini R and Morin D. A carbon monoxide-releasing molecule (CORM-3) uncouples mitochondrial respiration and modulates the production of reactive oxygen species. *Free Rad Biol Med* 50: 1556-1564, 2011.
 37. Mann BE. CO-Releasing Molecules: A Personal View. *Organometallics* 31: 5728-5735, 2012.
 38. McLean S, Begg R, Jesse HE, Mann BE, Sanguinetti G and Poole RK. Analysis of the bacterial response to Ru(CO)₃Cl(glycinate) (CORM-3) and the inactivated compound identifies the role played by the ruthenium compound and reveals sulfur-containing

- species as a major target of CORM-3 action. *Antiox Redox Signal* 19: 1999-2012, 2013.
39. McLean S, Mann BE and Poole RK. Sulfite species enhance carbon monoxide release from CO-releasing molecules: Implications for the deoxymyoglobin assay of activity. *Anal Biochem* 427: 36-40, 2012.
40. Murray TS, Okegbe C, Gao Y, Kazmierczak BI, Motterlini R, Dietrich LEP and Bruscia EM. The carbon monoxide releasing molecule CORM-2 attenuates *Pseudomonas aeruginosa* biofilm formation. *PLOS ONE* 7: e35499, 2012.
41. Nagel C, McLean S, Poole RK, Braunschweig H, Kramer T and Schatzschneider U. Introducing $[\text{Mn}(\text{CO})_3(\text{tpa-}k^3\text{N})]^+$ as a novel photoactivatable CO-releasing molecule with well-defined iCORM intermediates - synthesis, spectroscopy, and antibacterial activity. *Dalton Trans* 43: 9986-9997, 2014.
42. Naseem R, Holland IB, Jacq A, Wann KT and Campbell AK. pH and monovalent cations regulate cytosolic free Ca^{2+} in *E. coli*. *Biochim Biophys Acta-Biomembranes* 1778: 1415-1422, 2008.
43. Nicholls DG and Ferguson SJ. *Bioenergetics 3* London: Academic Press; 2002.
44. Nightingale CH, Ambrose PG, Drusano GL and Murakawa T (Eds). *Antimicrobial Pharmacodynamics in Theory and Clinical Practice, Second Edition (Infectious Disease and Therapy)*: Informa Healthcare; 2007.
45. Nikaido H. Molecular basis of bacterial outer membrane permeability revisited. *Microbiol Mol Biol Rev* 67: 593-656, 2003.
46. Nobre LS, Al-Shahrour F, Dopazo J and Saraiva LM. Exploring the antimicrobial action of a carbon monoxide-releasing compound through whole-genome transcription profiling of *Escherichia coli*. *Microbiology* 155: 813-824, 2009.
47. Nomura T, Cox CD, Bavi N, Sokabe M and Martinac B. Unidirectional incorporation of a bacterial mechanosensitive channel into liposomal membranes. *FASEB J* 29: 4334-4345, 2015.
48. Odds FC. Synergy, antagonism, and what the chequerboard puts between them. *J Antimicrob Chemother* 52: 1, 2003.
49. Outten CE and O'Halloran TV. Femtomolar sensitivity of metalloregulatory proteins controlling zinc homeostasis. *Science* 292: 2488-2492, 2001.
50. Papapetropoulos A, Foresti R and Ferdinandy P. Pharmacology of the 'gasotransmitters' NO, CO and H₂S: translational opportunities. *Br J Pharmacol* 172: 1395-1396, 2015.
51. Patzer SI and Hantke K. The ZnuABC high-affinity zinc uptake system and its regulator Zur in *Escherichia coli*. *Mol Microbiol* 28: 1199-1210, 1998.
52. Poole RK. The influence of growth substrate and capacity for oxidative phosphorylation on respiratory oscillations in synchronous cultures of *Escherichia coli* K12. *J Gen Microbiol* 99: 369-377, 1977.

Wareham: Antibacterial activities of a manganese CORM

53. Quan S, Hiniker A, Collet JF and Bardwell JC. Isolation of bacteria envelope proteins. *Methods Mol Biol* 966: 359-66, 2013.
54. Radchenko MV, Tanaka K, Waditee R, Oshimi S, Matsuzaki Y, Fukuhara M, Kobayashi H, Takabe T and Nakamura T. Potassium/proton antiport system of *Escherichia coli*. *J Biol Chem* 281: 19822-19829, 2006.
55. Raivio TL. Envelope stress responses and Gram-negative bacterial pathogenesis. *Mol Microbiol* 56: 1119-28, 2005.
56. Rana N, McLean S, Mann BE and Poole RK. Interaction of the carbon monoxide-releasing molecule Ru(CO)₃Cl(glycinate) (CORM-3) with *Salmonella enterica* serovar Typhimurium: in situ measurements of carbon monoxide binding by integrating cavity dual-beam spectrophotometry. *Microbiology* 160: 2771-9, 2014.
57. Sanguinetti G, Lawrence ND and Rattray M. Probabilistic inference of transcription factor concentrations and gene-specific regulatory activities. *Bioinformatics* 22: 2775-2781, 2006.
58. Sanguinetti G, Rattray M and Lawrence ND. A probabilistic dynamical model for quantitative inference of the regulatory mechanism of transcription. *Bioinformatics* 22: 1753-1759, 2006.
59. Santos-Silva T, Mukhopadhyay A, Seixas JD, Bernardes GJL, Romao CC and Romao MJ. CORM-3 reactivity toward proteins: The crystal structure of a Ru(II) dicarbonyl-lysozyme complex. *J Am Chem Soc* 133: 1192-1195, 2011.
60. Sawle P, Foresti R, Mann BE, Johnson TR, Green CJ and Motterlini R. Carbon monoxide-releasing molecules (CO-RMs) attenuate the inflammatory response elicited by lipopolysaccharide in RAW264.7 murine macrophages. *Br J Pharmacol* 145: 800-810, 2005.
61. Sims PJ, Waggoner AS, Wang CH and Hoffman JF. Studies on the mechanism by which cyanine dyes measure membrane potential in red blood cells and phosphatidylcholine vesicles. *Biochemistry* 13: 3315-3330, 1974.
62. Soupene E, King N, Lee H and Kustu S. Aquaporin Z of *Escherichia coli*: Reassessment of its regulation and physiological role. *J Bacteriol* 184: 4304-4307, 2002.
63. Southam HM, Butler JA, Chapman JA and Poole RK. The microbiology of ruthenium complexes. In: *Adv Microb Physiol*. edited by Poole RK. London: Elsevier; 2017. pp. 1-?
64. Strateva T and Yordanov D. *Pseudomonas aeruginosa* - a phenomenon of bacterial resistance. *J Med Microbiol* 58: 1133-48, 2009.
65. Strop P, Bass R and Rees DC. Prokaryotic mechanosensitive channels. *Adv Protein Chem* 63: 177-209, 2003.
66. Sugiura A, Hirokawa K, Nakashima K and Mizuno T. Signal-sensing mechanisms of the putative osmosensor KdpD in *Escherichia coli*. *Mol Microbiol* 14: 929-38, 1994.
67. Tinajero-Trejo M, Rana N, Nagel C, Jesse HE, Smith TW, Wareham LK, Hippler M, Schatzschneider U and Poole RK. Antimicrobial activity of the manganese

- photoactivated carbon monoxide-releasing molecule $\text{Mn}(\text{CO})_3(\text{tpa-}\kappa\text{-n-3})^+$ against a pathogenic *Escherichia coli* that causes urinary infections. *Antiox Redox Signal* 24: 765-780, 2016.
68. Totsika M, Beatson SA, Sarkar S, Phan MD, Petty NK, Bachmann N, Szubert M, Sidjabat HE, Paterson DL, Upton M and Schembri MA. Insights into a multidrug resistant *Escherichia coli* pathogen of the globally disseminated ST131 lineage: genome analysis and virulence mechanisms. *PLOS ONE* 6: e26578, 2011.
69. Wareham LK, Begg R, Jesse HE, van Beilen JWA, Ali S, Svistunenko D, McLean S, Hellingwerf KJ, Sanguinetti G and Poole RK. Carbon monoxide gas is not inert, but global, in its consequences for bacterial gene expression, iron acquisition, and antibiotic resistance. *Antiox Redox Signal* 24: 1013-1028, 2016.
70. Wareham LK, Poole RK and Tinajero-Trejo M. CO-releasing metal carbonyl compounds as antimicrobial agents in the post-antibiotic era. *J Biol Chem* 290: 18999-19007, 2015.
71. WHO. 2017. Global priority list of antibiotic-resistant bacteria to guide research, discovery, and development of new antibiotics. <http://www.who.int/medicines/publications/global-priority-list-antibiotic-resistant-bacteria/en/>.
72. Wilson JL, Bouillaud F, Almeida AS, Vieira HL, Ouidja MO, Dubois-Rande JL, Foresti R and Motterlini R. Carbon monoxide reverses the metabolic adaptation of microglia cells to an inflammatory stimulus. *Free Rad Biol Med* 104: 311-323, 2017.
73. Wilson JL, Jesse HE, Hughes BM, Lund V, Naylor K, Davidge KS, Cook GM, Mann BE and Poole RK. $\text{Ru}(\text{CO})_3\text{Cl}(\text{glycinate})$ (CORM-3): a CO-releasing molecule with broad-spectrum antimicrobial and photosensitive activities against respiration and cation transport in *Escherichia coli*. *Antioxid Redox Signal* 19: 497-509, 2013.
74. Wilson JL, Wareham LK, McLean S, Begg R, Greaves S, Mann BE, Sanguinetti G and Poole RK. CO-Releasing molecules have nonheme targets in bacteria: transcriptomic, mathematical modeling and biochemical analyses of CORM-3 [$\text{Ru}(\text{CO})\text{Cl}(\text{glycinate})$] Actions on a heme-deficient mutant of *Escherichia coli*. *Antioxid Redox Signal* 23: 148-162, 2015.
75. Wood JM. Osmosensing by bacteria: Signals and membrane-based sensors. *Microbiol Mol Biol Rev* 63: 230-262, 1999.

Table 1 Interactions of CORM-401 with antibiotics having different modes of action. FIC values (calculated as described in Methods) are shown for CORM-401 in combination with the selected antibiotics. Minimal inhibitory concentrations (MIC) are expressed as $\mu\text{g ml}^{-1}$. The description of the interaction follows the recommendation of Odds (48).

Antibiotic	FIC _{antibiotic} [*]	FIC _{CORM} [°]	$\Sigma\text{FIC} = \text{FIC}_{\text{antibiotic}} + \text{FIC}_{\text{CORM}}$	CORM/antibiotic interaction
<i>E. coli</i> strain MG1655				
Doxycycline	0.25	0.66	0.91	No interaction
Trimethoprim	0.12	0.42	0.54	No interaction
Novobiocin	0.33	0.33	0.66	No interaction
Cefotaxime	0.12	0.66	0.78	No interaction
<i>E. coli</i> strain EC958				
Colistin	0.5	0.06	0.56	No interaction
Doxycycline	0.5	0.13	0.63	No interaction
Gentamicin	1.0	0.03	1.03	No interaction

*MIC of antibiotic in combination/MIC of antibiotic alone

°MIC of CORM in combination/MIC of CORM alone

Figure legends

FIG. 1. CO release from CORM-401 in bacterial growth medium. Assays were performed in Evans minimal medium (with glucose as sole carbon source) in the presence of excess dithionite at 37 °C. **A)** CO difference spectra showing the conversion of myoglobin (15 µM) to the carbonmonoxy-ferrous species in the presence of 3 µM CORM-401. **B)** Time course of CO release from CORM-401 in medium at 37 °C. Under these conditions, CORM-401 releases 2.5 mole equivalent of CO with a $t_{1/2}$ of 4.5 min. Data are means of three biological repeats ± SEM.

FIG. 2. CORM-401 inhibits growth of *E. coli* and is bactericidal to glucose-grown cells. Cells were grown to exponential phase before addition of CORM at time = 0. **A)** Growth supplemented with glucose in the absence of CORM-401 (closed circles) and after addition of 10 µM (open circles), 67 µM (open triangles) and 500 µM (squares) CORM-401. **B)** Growth supplemented with succinate, symbols as above. **Insets in A, B)** Growth with 500 µM DTC/MnSO₄ on glucose and succinate showed no deleterious effect on growth of cells. **C)** Viable counts at hourly intervals of cells growing on glucose. **D)** Viable counts of cells growing on succinate. Following the addition of CORM-401 to *E. coli* MG1655 at OD₆₀₀ 0.6, cells were incubated for 90 min before sampling * indicates $P \leq 0.008$. Data are representative of three biological repeats.

FIG. 3 Manganese levels in cells treated with CORM-401 or control compounds

Wareham: Antibacterial activities of a manganese CORM

1
2
3 A) Intracellular Mn levels in *E. coli* grown on 20 mM glucose (closed circles) or 20 mM
4 succinate (open circles) then treated with CORM-401 (final concentration 67 μ M); $n = 3$, \pm SEM.
5
6
7
8 B) Localization of Mn following addition of 67 μ M CORM-401 (grey bars) to *E. coli* MG1655
9 sub-cellular fractions. Black bars show Mn amounts in each fraction with no additional CORM-
10 401. C) Mn levels in cells incubated for 80 min in the presence (black bars) or absence (gray
11 bars) of a saturated CO solution (approx. 500 μ M, final concentration). D) Mn levels in cells
12 prior to additions (black bars) or after adding 500 μ M MnSO₄ +/- 67 mM DTC. $n = 3$, \pm SEM.
13
14
15
16
17
18
19
20 Note the different scales in A-D.
21
22
23
24

25 **FIG. 4. Functional categories of genes affected by CORM-401 under aerobic and anaerobic**
26 **conditions.** Genes are grouped according to functional categories. The bars show the percentage
27 of genes in each group that exhibit significantly altered gene expression (i.e. where fold changes
28 are ≥ 2 and ≤ 0.5) under **A)** aerobic conditions and **B)** anaerobic conditions. Gene changes are
29 shown as genes up-regulated (right, black bars) and down-regulated (left, grey bars) in each
30 group.
31
32
33
34
35
36
37
38
39
40

41 **FIG. 5. TFInfer correlation profiles (coherence plots) showing transcription factors**
42 **involved in the response to CORM-401 vs. CO gas in *E. coli* cells.** The x-coordinate of each
43 point represents the 'profile difference' between CORM-401 or CO treatments, computed as 1
44 minus the absolute Pearson correlation coefficient between the two profiles); the y-coordinate
45 represents the change in magnitude of the response (computed as the difference of the norm of
46 the two profiles). Data from aerobic (**A**, top) and anaerobic (**B**, bottom) are shown. Transcription
47 factors (TFs) whose response is similar with both CORM-401 and CO gas, both in magnitude
48
49
50
51
52
53
54
55
56
57
58
59
60

and kinetics, will be located near the origin of each coherence plot in quadrant C, while TFs in quadrant B of each plot respond differently in both kinetics and amplitude. For example, CpxR, both aerobically and anaerobically, has a similar response in terms of the shape of the profile but different magnitudes in A and B, while ArcA (in **A**) and ArgR (in **B**) show similar magnitudes but major differences in response profiles.

FIG. 6. Differential expression of genes involved in the respiratory chains both aerobically and anaerobically in response to 67 μ M CORM-401. The heat map quantifies the changes elicited in selected genes; the ‘heat scale’ at the *right* is expressed as the natural logarithm of the fold change. To see this illustration in color, the reader is referred to the web version of this article at www.liebertpub.com/ars.

FIG. 7. CO released from CORM-401 binds terminal oxidases in whole cells but exhibits “uncoupler-like” activity on respiration. **A)** Cells were grown in LB media to exponential phase and concentrated in PBS to an OD of ~ 55 . CORM-401 was added to a final concentration of 100 μ M. CO difference spectra were recorded over 15 min; arrows show the direction of absorbance increase or decrease in successive scans. **B)** Membrane particles (60 μ g protein/ml) from wild type *E. coli* were added to a closed electrode chamber. Respiration was stimulated by addition of NADH and when air saturation had reached $\sim 75\%$ of the initial (arrow), CO saturated solution (dashed line) or CORM-401 (final concentration 100 μ M) were added (grey dotted line). Respiration of membranes in the absence of any compounds was followed as a control (solid line). **C)** Cells were grown to mid-exponential phase (OD_{600nm} ~ 0.6) in Evans medium, and re-suspended in Tris-HCl buffer pH 7.4 before analysis in an open oxygen electrode. Where indicated by arrows, glucose was added to stimulate respiration and cells respired until a steady-

state was reached before addition of 100 μ M CORM-401. Inset shows 10 μ M CCCP added under equivalent conditions. **D)** Partial inhibition of respiration was observed at low oxygen tensions when CORM-401 was added twice (arrows marked 'CORM-401'). In C and D, KCN was added at the arrows at the end of the experiment to the chamber to a final concentration of 1 mM to fully inhibit respiration. All data are representative of 3 biological repeats.

FIG. 8. CORM-401 and the classical uncoupler CCCP cause polarization of the membrane in whole cells. *E. coli* cells were grown to exponential phase and resuspended in 5 mM HEPES buffer to a final OD₆₀₀ of 0.6. Cells were incubated with 0.1 M KCl and 10 mM glucose before incubation with 0.4 μ M DiSC3(5). Additions were as follows: **A)** 1 μ M valinomycin (val); **B)** 50 μ M CO (solid line) or buffer (dotted line); **C)** 50 μ M CORM-401; **D)** 1 μ M CCCP; Trace **E)** shows additions of 1 μ M valinomycin followed by 50 μ M CORM-401; **F)** show additions of 1 μ M valinomycin and then 1 μ M CCCP. Results are representative of 3 independent, biological repeats, where net changes in fluorescence were equivalent across all repeats. Fluorescence changes (ΔF) are expressed as arbitrary units (A.U.).

FIG. 9. Differential expression of gene involved in osmoregulation. The heat map quantifies the changes elicited in selected genes both aerobically and anaerobically in response to 67 μ M CORM-401. The 'heat scale' at the right is expressed as the natural logarithm of the fold change. To see this illustration in color, the reader is referred to the web version of this article at www.liebertpub.com/ars.

FIG. 10. Potassium and zinc levels fall after CORM-401 addition. *E. coli* cells were grown to exponential phase in Evans medium supplemented with 20 mM glucose. Samples were taken

immediately prior to ($t = 0$) and at time intervals after 67 μM CORM-401 addition (final concentration). Cell pellets were analysed using ICP-MS. **A)** Intracellular potassium and iron levels; potassium falls significantly between $t = 0$ and $t = 80$ ($P = 0.03$). **B)** Zinc and copper levels; zinc levels fall between $t = 0$ and $t = 80$. $n = 3 \pm \text{SEM}$.

FIG. 11. Differential expression of genes implicated in general stress responses, metal ion stress and cell envelope stress. The color-scale bar shows mean fold changes in individual genes of WT *E. coli* both aerobically and anaerobically in response to 67 μM CORM-401. The ‘heat scale’ at the right is expressed as the natural logarithm of the fold change. To see this illustration in color, the reader is referred to the web version of this article at www.liebertpub.com/ars.

FIG. 12. CORM-401 leads to up-regulation of cellular stress responses but does not perturb the outer membrane of *E. coli*. **A)** Coomassie-stained SDS gel of soluble fractions used in western blotting illustrates equal loading of protein. Molecular mass markers (kDa) are shown on the left. **B)** A typical Western blot of subcellular fractions is shown in the absence (lane 1) and presence of 67 μM DTC/ MnSO_4 (lane 2) or 67 μM CORM-401 (lane 3) for 2 h with anti-CpxP and anti-Spy antibodies. Data shown are representative of 3 biological replicates. **C)** Cells were re-suspended in PBS then exposed to NPN alone (black bar), NPN + 3% triton (positive control) (grey bar) or 100 μM CORM-401 for increasing time periods (as labeled). All concentrations given are final concentrations in the fluorescence cuvette. $n = 3 \pm \text{SEM}$.

FIG. 13. A growth screen of pathogens isolated from clinical infections show varying susceptibility to CORM-401. Strains were grown in Evans medium with glucose to early-

Wareham: Antibacterial activities of a manganese CORM

exponential phase prior to the addition of 500 μM CORM-401 (closed circles, addition indicated by arrows) or the equivalent volume of PBS (open circles). Growth was monitored throughout, $n=3 \pm \text{SD}$.

FIG. 14. Schematic diagram of a hypothesis for the antimicrobial effects of CORM-401.

CORM-401 (structure shown at bottom left), administered extracellularly, is transported inwards to the cytoplasm either by diffusion (1) or by an unidentified transporter (2). Within the cell, CO is released (3) leaving a metal co-ligand fragment ('iCORM'). CORM accumulates to very high levels (4), perhaps as a result of the maintenance of a concentration gradient, following conversion of the CORM (outside) to iCORM (inside). CORM-401 and/or its breakdown products elicit major transcriptional changes (5), reflected in altered protein synthesis/function. CO, whether released from CORM within cells or following gas diffusion from outside (6), binds to oxidases (O) and partly inhibits aerobic NADH oxidation via flavins (F) and quinones (Q) (7). This perturbs the protonmotive force, which is matched by enhanced respiration leading to membrane polarization, which in turn drives further uptake. Translocation of cations (M^{n+}) such as K^+ or Zn(II) is shown (8).

SUPPLEMENTARY TABLE 1. List of the thirty most highly regulated genes, both aerobically and anaerobically. Values shown are fold changes relative to the pre-CORM culture sampled at the time points shown.

SUPPLEMENTARY FIG. S1. CO release from CORM-401 in 0.1 M KPi (pH 7.4) at 37 or 20 °C. Assays were performed in the presence of excess dithionite with myoglobin (20 μM) and 5 μM CORM-401. Under these conditions, CORM-401 releases 2.4 mole equivalent of CO with a $t_{1/2}$ of 5 min. $n = 3 \pm \text{SEM}$.

SUPPLEMENTARY FIG. S2. TFInfer correlation profiles (coherence plots) showing transcription factors involved in the response to CORM-401 vs. CO gas in *E. coli* cells. The x-coordinate of each point is presented with error bars and represents the ‘profile difference’ between CORM-401 or CO treatments, computed as 1 minus the absolute Pearson correlation coefficient between the two profiles); the y-coordinate represents the change in magnitude of the response (computed as the difference of the norm of the two profiles). Data from aerobic (A, top) and anaerobic (B, bottom) are shown. Transcription factors (TFs) whose response is similar with both CORM-401 and CO gas, both in magnitude and kinetics, will be located near the origin of each coherence plot in quadrant c, while TFs in quadrant b of each plot respond differently in both kinetics and amplitude. For example, CpxR, both aerobically and anaerobically, has a similar response in terms of the shape of the profile but different magnitudes in A and B, while ArcA (in A) and ArgR (in B) show similar magnitudes but major differences in response profiles.

SUPPLEMENTARY FIG. S3. Differential expression of genes , both aerobically and anaerobically, in response to 67 μ M CORM-401, involved in (A) the respiratory chains, (B) osmoregulation and (C) general stress responses, metal ion stress and cell envelope stress.

Values within each cell are fold changes in transcript levels relative to the no-CORM condition.

The heat map (above) also quantifies the changes elicited in selected genes.

SUPPLEMENTARY FIG. S4. CORM-401 enhances the antimicrobial effects of cefotaxime and trimethoprim with additive effects on growth and viability. In A and B, bacterial growth was followed in Evans medium with glucose until $OD_{600nm} \sim 0.3$ was reached. CORM-401 and antibiotics were then added to the cultures; OD readings and samples for viability were taken at regular intervals. In A (cefotaxime) and B (trimethoprim), squares show control cultures, triangles are antibiotic alone ($1 \mu\text{g ml}^{-1}$), inverted triangles are CORM-401 alone ($100 \mu\text{M}$), and diamonds are antibiotic and CORM combined. In C (cefotaxime) and D (trimethoprim), black columns show control cultures, diagonal-hatched bars are antibiotic alone ($1 \mu\text{g ml}^{-1}$), horizontally striped bars are CORM-401 alone ($100 \mu\text{M}$), and open bars are antibiotic and CORM combined. $n = 3 \pm \text{SD}$.

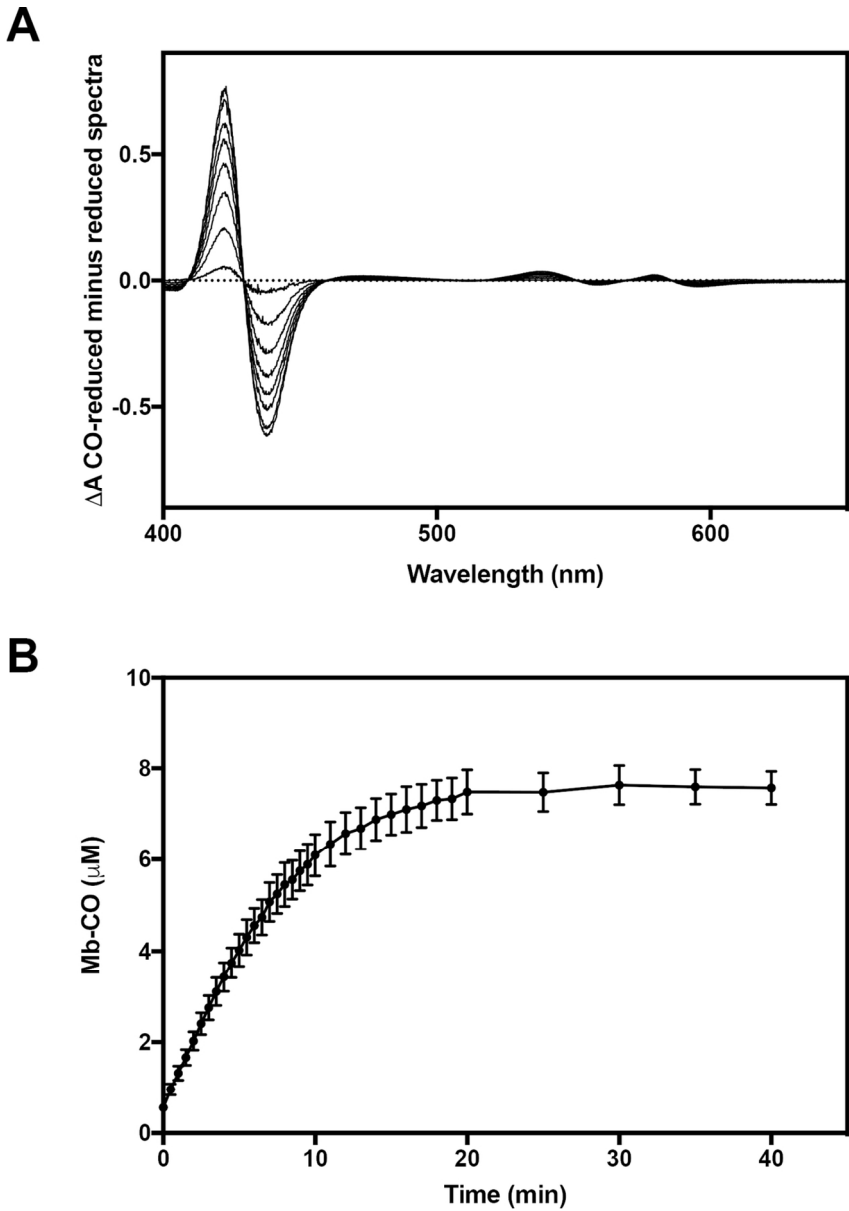


Fig. 1

106x152mm (300 x 300 DPI)

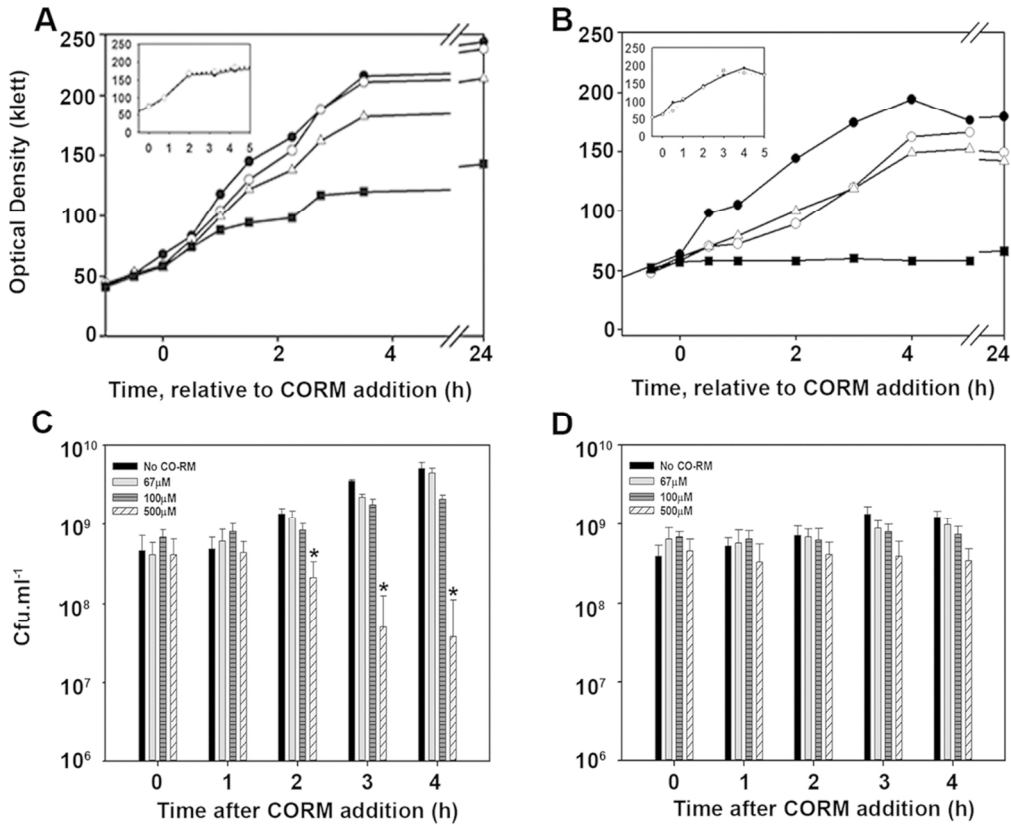


Fig. 2

122x100mm (300 x 300 DPI)

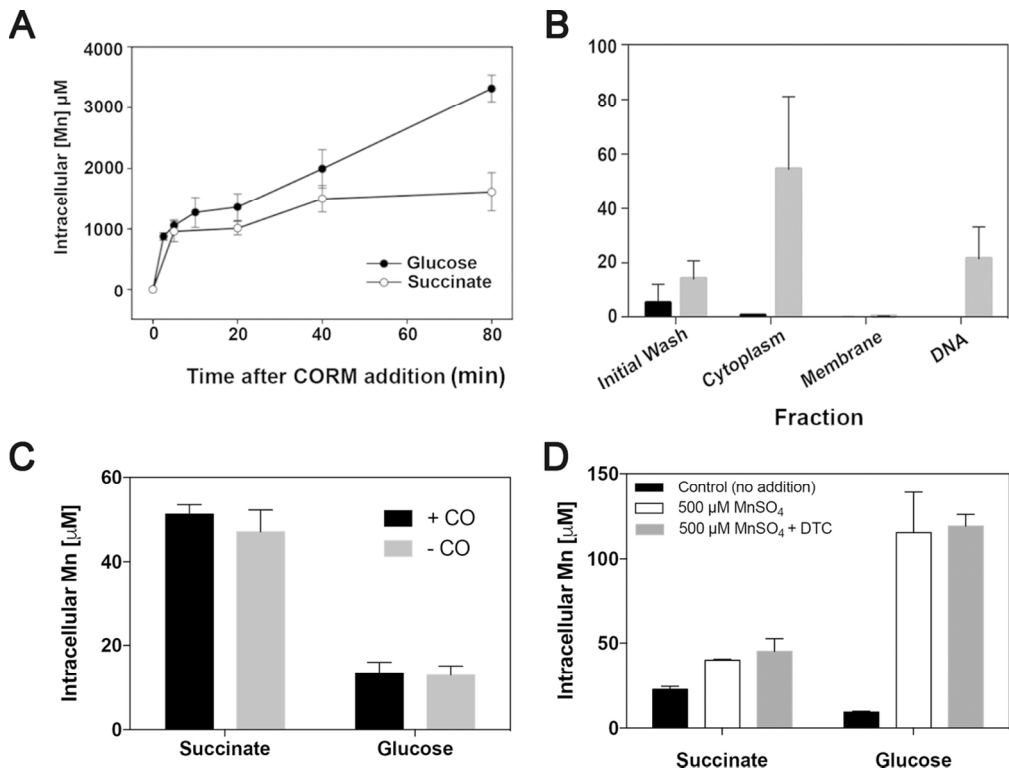


Fig. 3

113x86mm (300 x 300 DPI)

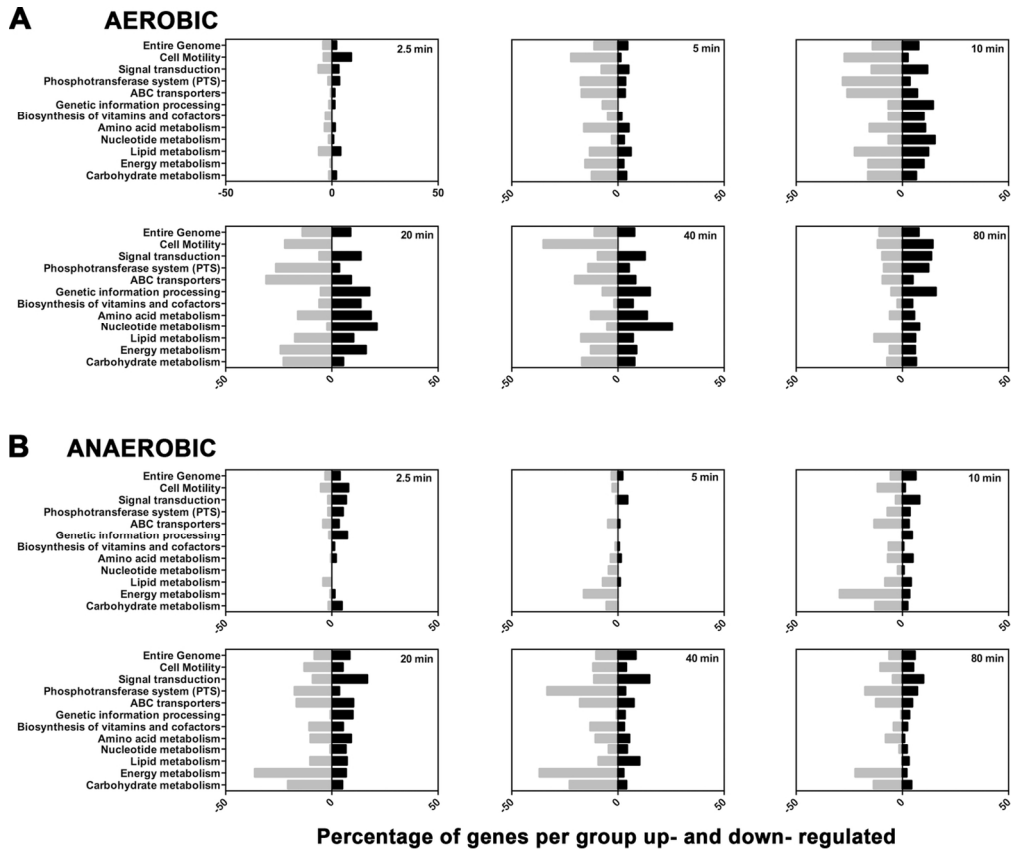


Fig. 4

126x105mm (300 x 300 DPI)

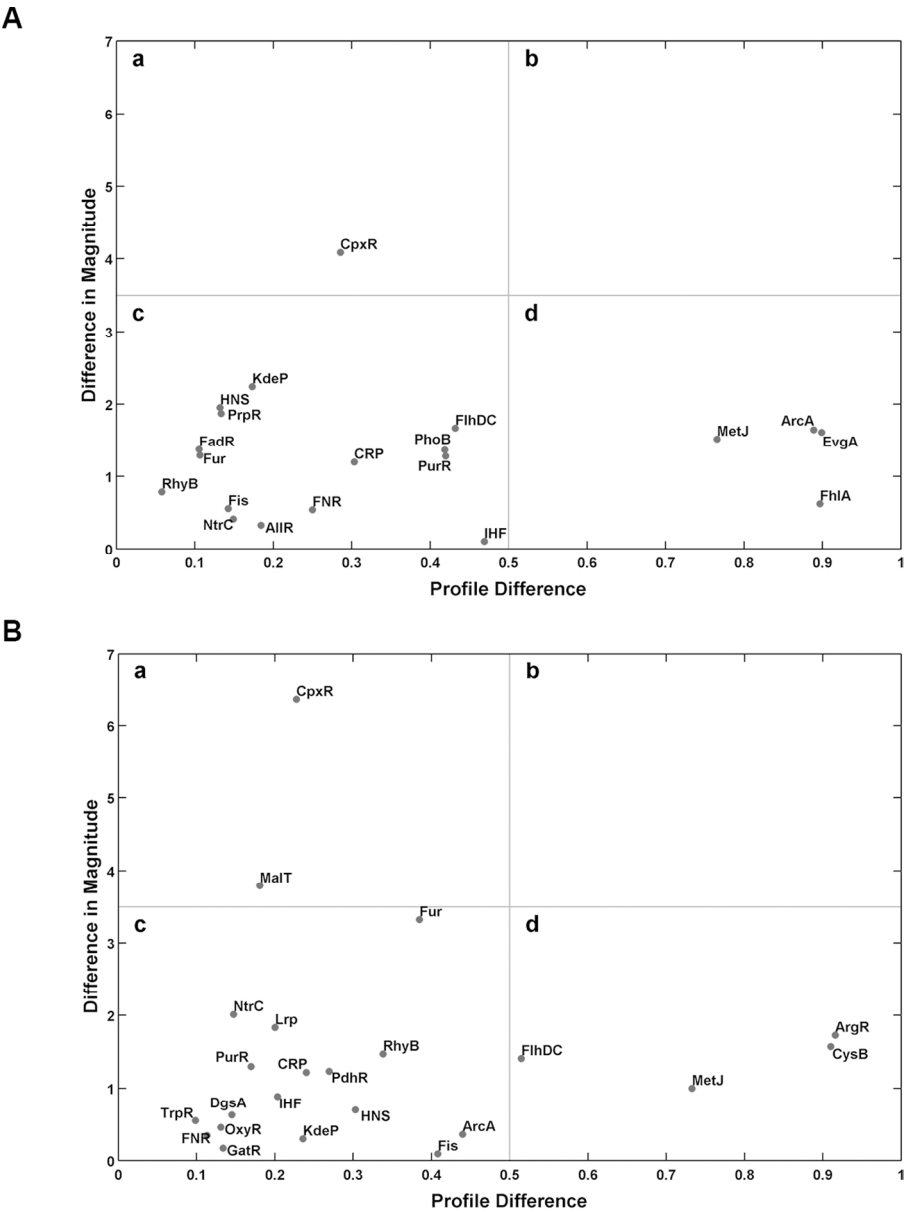


Fig. 5

150x200mm (209 x 209 DPI)



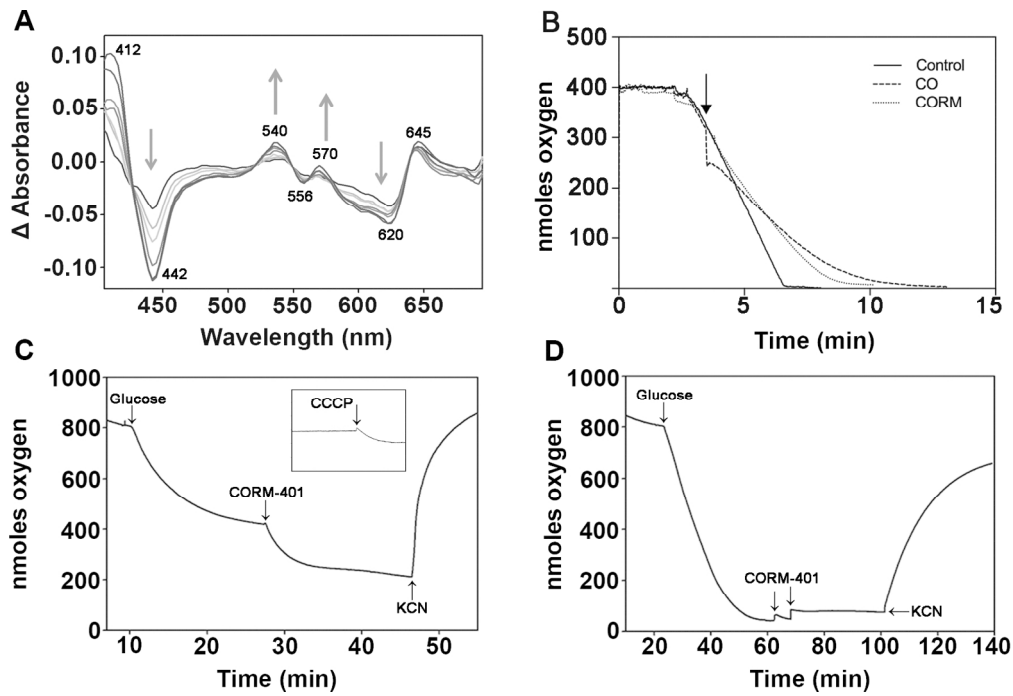


Fig. 7

150x102mm (299 x 299 DPI)

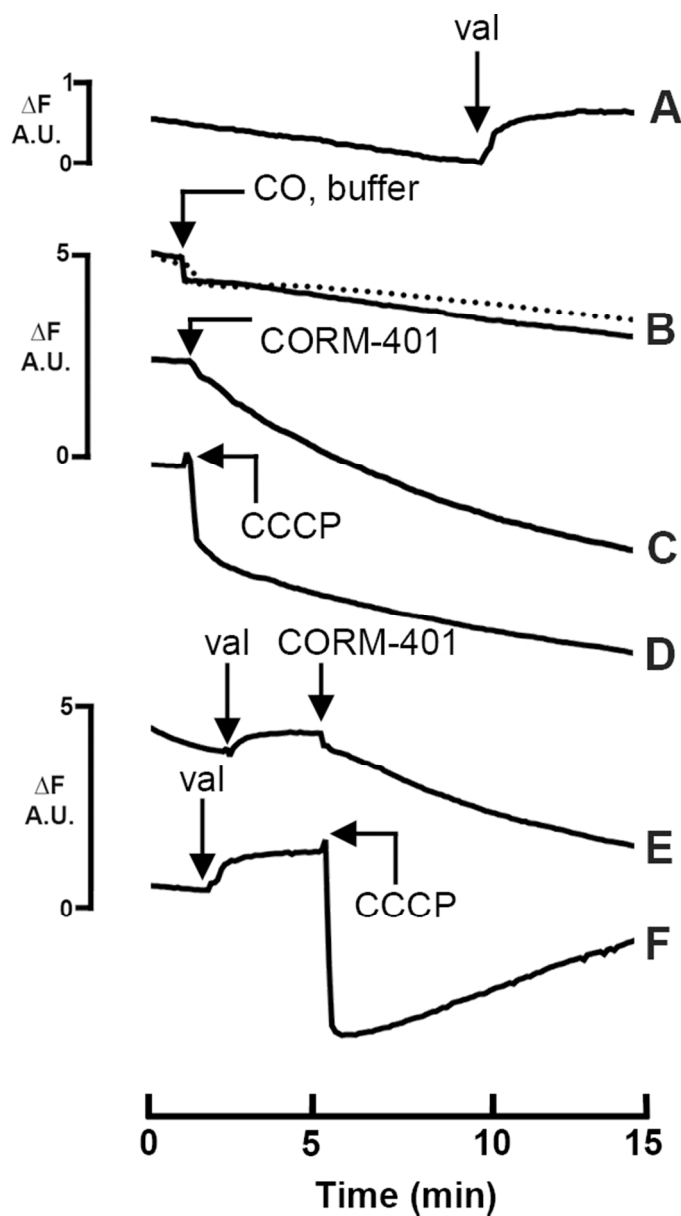


Fig. 8

75x134mm (209 x 209 DPI)



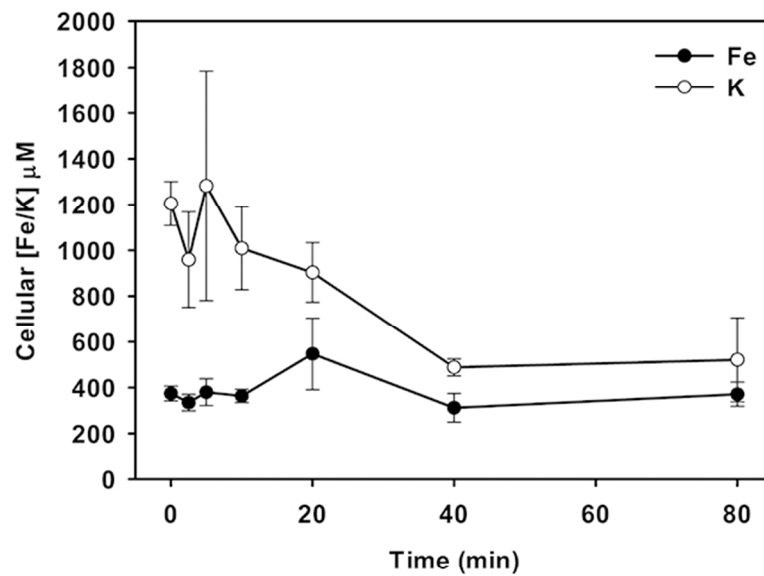
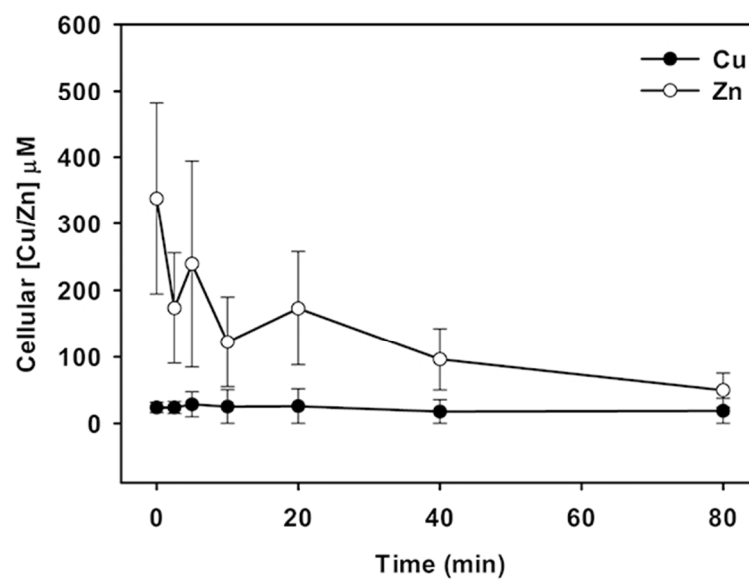
A**B**

Fig. 10

75x103mm (249 x 249 DPI)

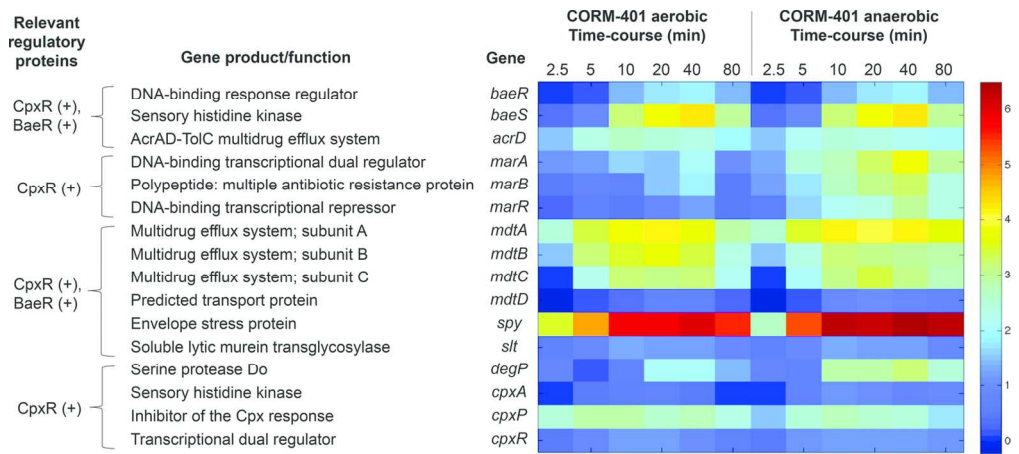


Fig. 11

66x29mm (600 x 600 DPI)

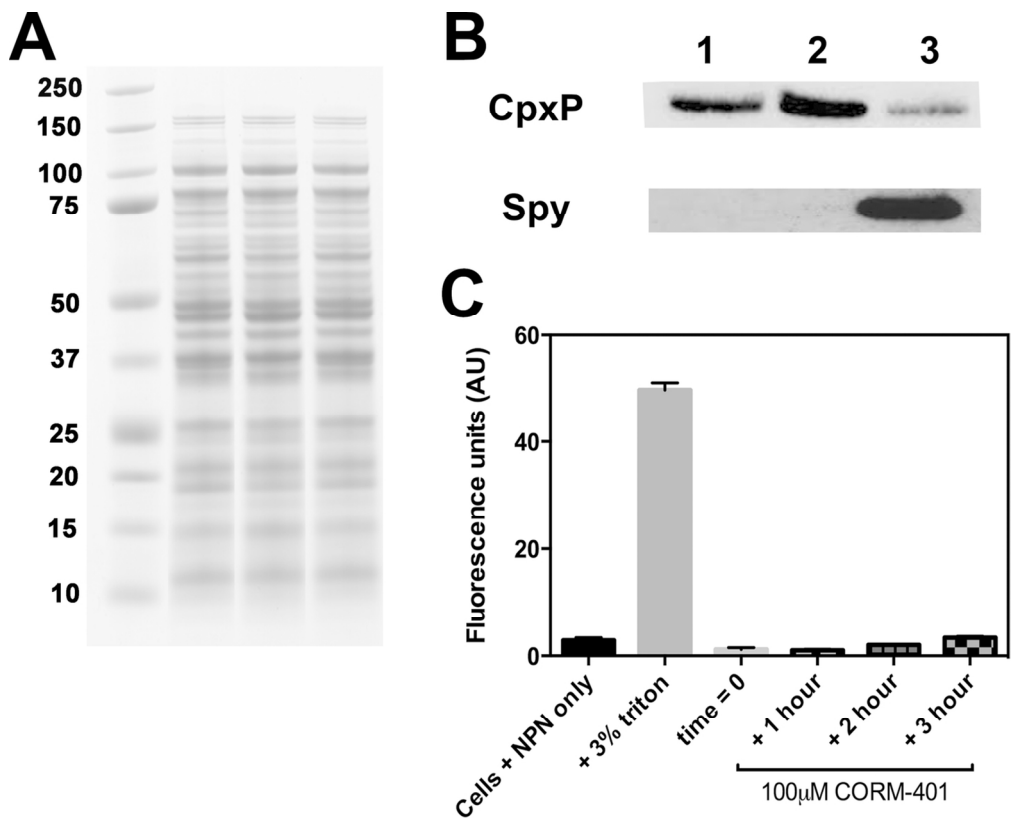


Fig. 12 (revised)

120x97mm (300 x 300 DPI)

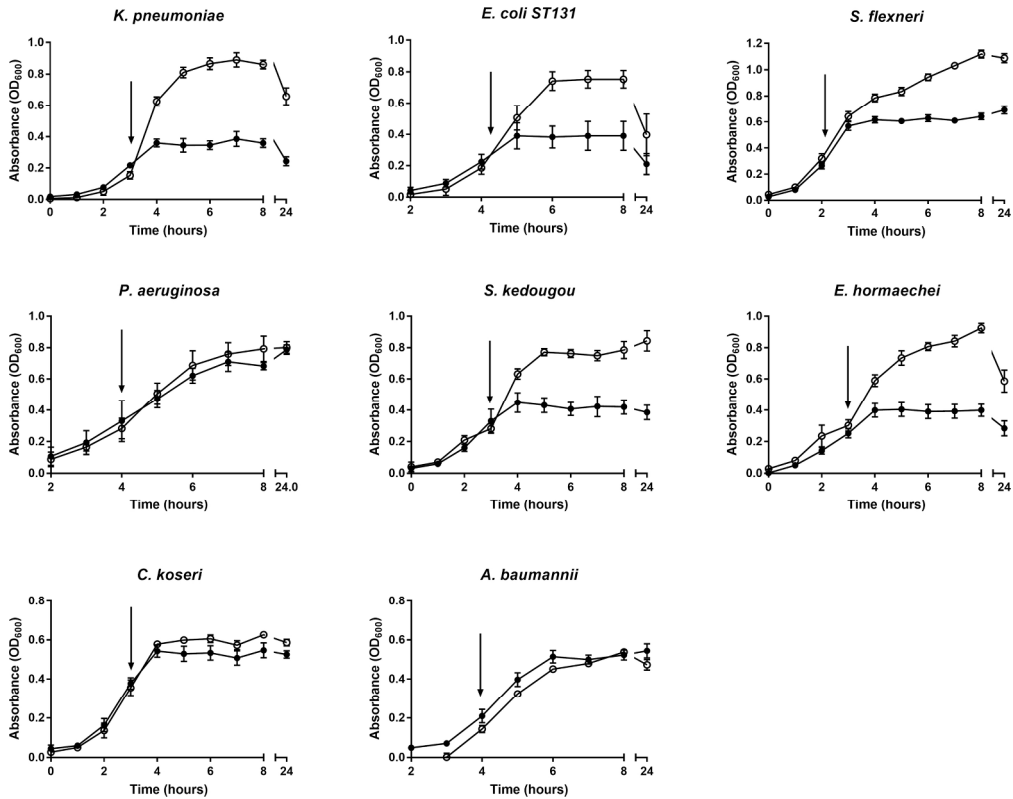


Fig. 13

109x86mm (600 x 600 DPI)

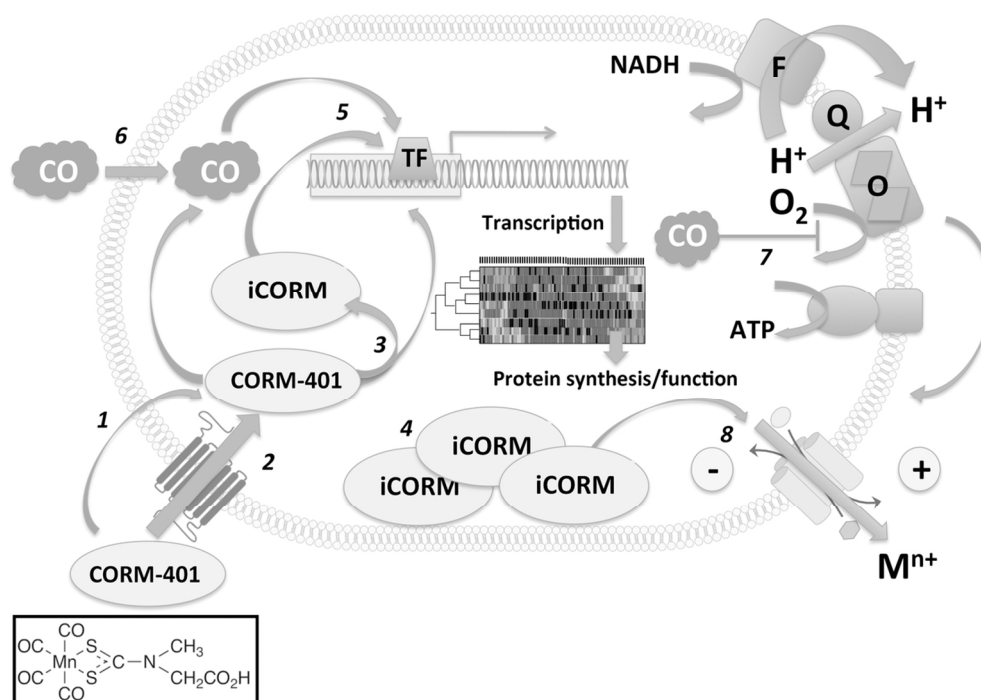
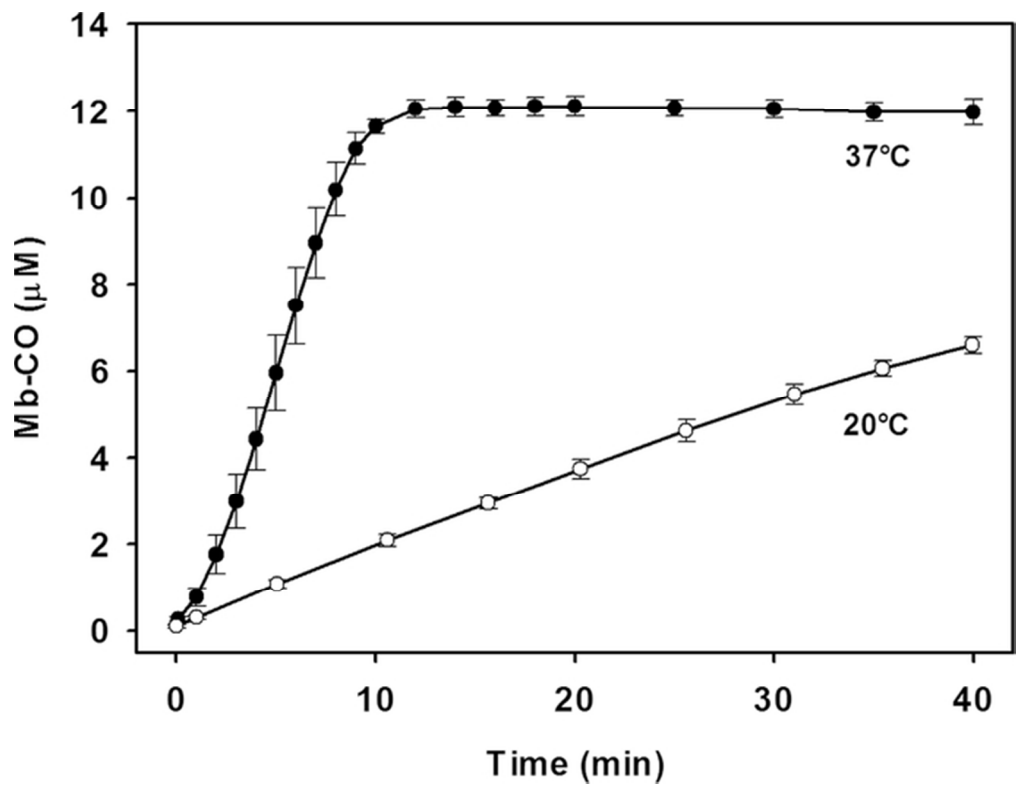


Fig. 14

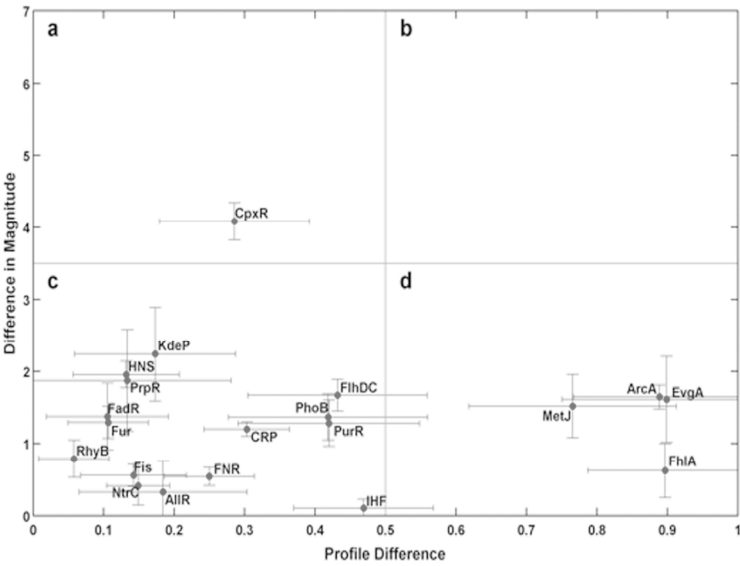
112x84mm (300 x 300 DPI)



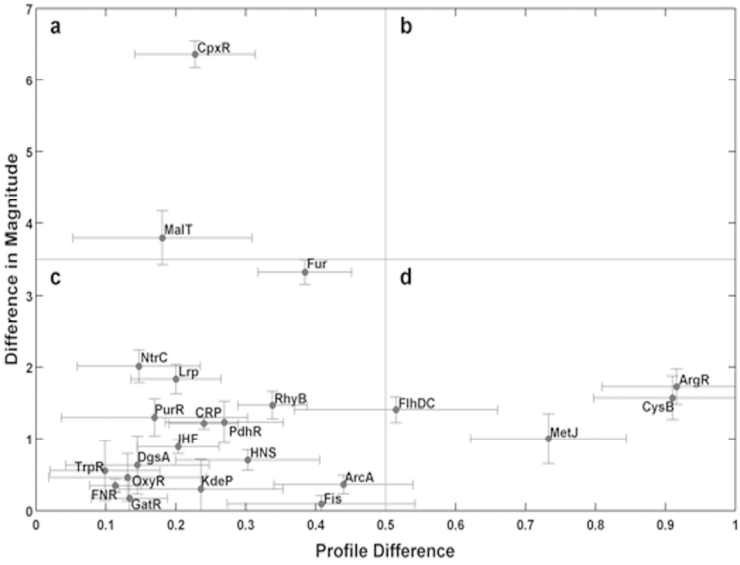
Supplementary Fig. 1

57x44mm (300 x 300 DPI)

A



B



Supplementary Fig. 2

150x210mm (278 x 278 DPI)

A

		Fold change down-regulated						Fold change up-regulated						
		30+	20-30	10-20	5-10	2-5	0.0	2-5	5-10	10-20	20-30	30+		
Gene	Function	Relevant regulatory proteins	CORM-401 AEROBIC						CORM-401 ANAEROBIC					
			Time						Time					
			2.5	5.0	10.0	20.0	40.0	80.0	2.5	5.0	10.0	20.0	40.0	80.0
<i>cyaA</i>	cytochrome <i>bo'</i> terminal oxidase subunit II	ArcA (-)			0.44	0.20			0.44	0.11	0.09	0.20		
<i>cyaB</i>	cytochrome <i>bo'</i> terminal oxidase subunit I	ArcA (-)				0.23			0.50	0.33	0.32	0.38		
<i>cyaC</i>	cytochrome <i>bo'</i> terminal oxidase subunit III	ArcA (-)				0.20				0.22	0.26	0.34		
<i>cyaD</i>	cytochrome <i>bo'</i> terminal oxidase subunit IV	ArcA (-)				0.20				0.23	0.21	0.26	0.48	
<i>cyaE</i>	heme o synthase	ArcA (-)				0.21				0.33	0.36	0.37	0.48	
<i>cyaD</i>	cytochrome <i>bd/f</i> terminal oxidase subunit I	ArcA (+), FNR (-)		2.88	2.42		2.86	3.07	2.01		0.32	0.26	0.25	0.38
<i>cyaB</i>	cytochrome <i>bd/f</i> terminal oxidase subunit II	ArcA (+) FNR (-)		2.54	2.37	2.07	2.83	2.70			0.42	0.30	0.22	0.39
<i>nuoA</i>	NADH:ubiquinone oxidoreductase I	ArcA (-), FNR (-)		0.49							0.39	0.29	0.27	0.39
<i>nuoB</i>	NADH:ubiquinone oxidoreductase I	ArcA (-), FNR (-)									0.43	0.39		
<i>nuoC</i>	NADH:ubiquinone oxidoreductase I	ArcA (-), FNR (-)				0.49					0.46	0.33	0.35	
<i>nuoE</i>	NADH:ubiquinone oxidoreductase I	ArcA (-), FNR (-)				0.44					0.45	0.33	0.34	
<i>nuoF</i>	NADH:ubiquinone oxidoreductase I	ArcA (-), FNR (-)									0.47	0.34	0.31	
<i>nuoG</i>	NADH:ubiquinone oxidoreductase I	ArcA (-), FNR (-)									0.50	0.32	0.26	0.48
<i>nuoH</i>	NADH:ubiquinone oxidoreductase I	ArcA (-), FNR (-)										0.41	0.30	
<i>nuoI</i>	NADH:ubiquinone oxidoreductase I	ArcA (-), FNR (-)										0.43	0.32	
<i>nuoJ</i>	NADH:ubiquinone oxidoreductase I	ArcA (-), FNR (-)										0.47	0.34	
<i>nuoK</i>	NADH:ubiquinone oxidoreductase I	ArcA (-), FNR (-)										0.39	0.31	
<i>nuoL</i>	NADH:ubiquinone oxidoreductase I	ArcA (-), FNR (-)										0.47	0.35	
<i>nuoM</i>	NADH:ubiquinone oxidoreductase I	ArcA (-), FNR (-)										0.35	0.28	0.48
<i>nuoN</i>	NADH:ubiquinone oxidoreductase I	ArcA (-), FNR (-)												
<i>ndh</i>	NADH dehydrogenase II	FNR (-)			2.27	2.50	2.45	2.04						

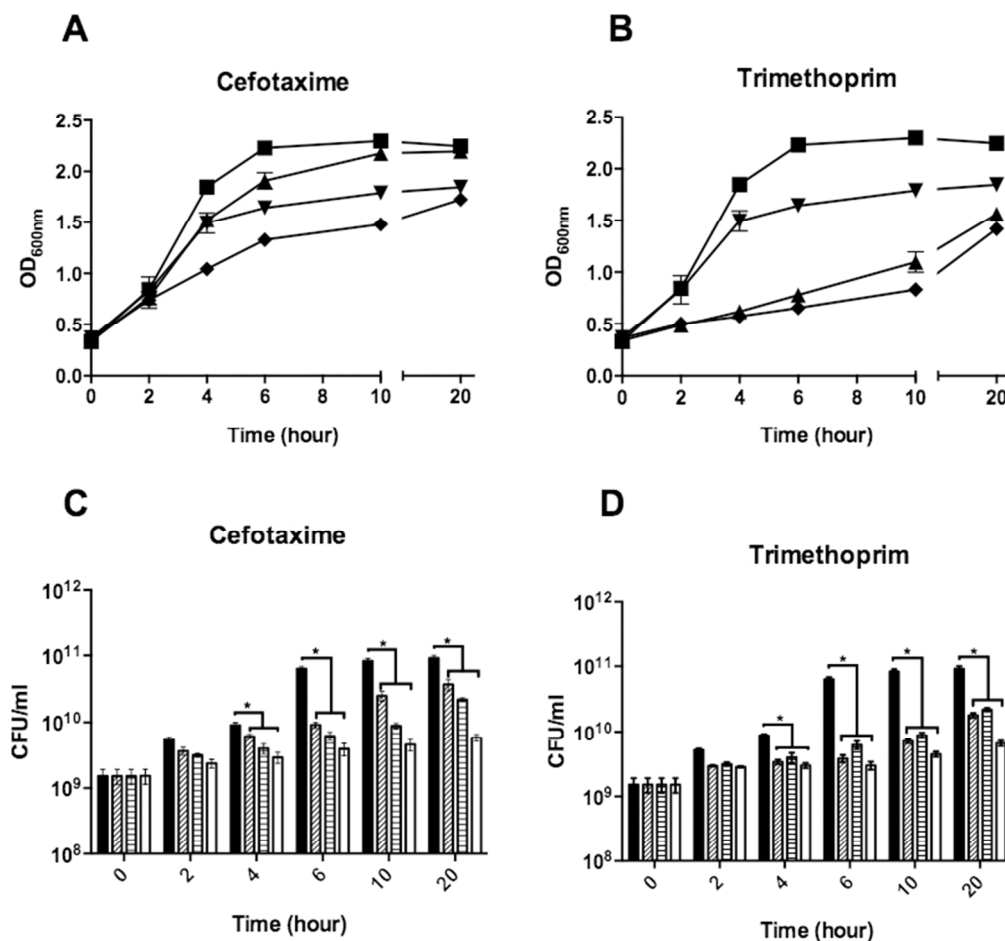
Gene		Product/Function	Relevant regulatory proteins	Fold change down-regulated						Fold change up-regulated					
				30+	20-30	10-20	5-10	2-5	0.0	2-5	5-10	10-20	20-30	30+	
				CORM-401 AEROBIC						CORM-401 ANAEROBIC					
				Time						Time					
			2.5	5.0	10.0	20.0	40.0	80.0	2.5	5.0	10.0	20.0	40.0	80.0	
<i>chaA</i>		Na ⁺ : K ⁺ /H ⁺ antiporter		2.2	7.0	14.4	9.8	5.8	4.1	2.2	6.4	12.1	9.5	11.7	4.2
<i>kdpA</i>		K ⁺ transporting ATPase subunit	KdpE (+)		2.9	11.3	15.6					2.1	2.3		
<i>kdpB</i>		K ⁺ transporting ATPase subunit	KdpE (+)			9.8	13.8	7.5	4.8			3.7	3.4	2.0	
<i>kdpC</i>		K ⁺ transporting ATPase subunit	KdpE (+)	0.4		32.8	33.8	18.2	5.5	2.8			4.6	2.8	
<i>kdpD</i>		regulator of the K ⁺ transporting ATPase					2.1						2.5		
<i>kdpE</i>		regulator of the K ⁺ transporting ATPase	KdpD-P (+)				2.7	2.6	2.0			2.4	2.3	2.0	
<i>kdpF</i>		K ⁺ transporting ATPase subunit			6.2	20.8	23.0		2.0		0.5				
<i>kefA (mscK)</i>		Potassium-dependent mechanosensitive channel					2.5	2.6					2.0		
<i>kefB</i>		K ⁺ - H ⁺ antiporter			0.3	0.1	0.1								
<i>kefC</i>		K ⁺ - H ⁺ antiporter													
<i>kefF</i>		Regulator of the Kef transporter					0.2								
<i>kefG</i>		Protein required for KefB activity				0.4	0.5								
<i>trkA</i>		K ⁺ transporter			2.3	2.6									
<i>znuA</i>		Zn ²⁺ ABC transporter	Zur (-)		2.6	6.5	11.2	10.0	5.2			3.4	4.3	7.2	6.4
<i>mscL</i>		mechanosensitive channel	RpoS (+)				0.4	0.4							
<i>mscS</i>		mechanosensitive channel	RpoS (+)			2.9	4.7	3.9				2.3	4.6	3.8	2.6
<i>aqpZ</i>		Aquaporin					0.3	0.4	0.4						
<i>ompC</i>		Outer membrane porin C	CpxR (-), OmpR (-)				2.1		3.1	2.5					
<i>ompF</i>		Outer membrane porin F	CpxR (-), OmpR (-)	0.5	0.2	0.2	0.0	0.1	0.2			0.2	0.0	0.0	0.0

C

		Fold change down-regulated						Fold change up-regulated						
		30+	20-30	10-20	5-10	2-5	0.0	2-5	5-10	10-20	20-30	30+		
Gene	Product/Function	Relevant regulatory proteins	CORM-401 AEROBIC CONDITIONS						CORM-401 ANAEROBIC CONDITIONS					
			Time						Time					
			2.5	5.0	10.0	20.0	40.0	80.0	2.5	5.0	10.0	20.0	40.0	80.0
<i>baeR</i>	DNA-binding response regulator	CpxR (+), BaeR (+)			4.2	5.9	6.8	4.3			3.7	5.3	4.8	3.5
<i>baeS</i>	Sensory histidine kinase	CpxR (+), BaeR (+)		2.3	25.1	45.4	67.4	19.7			31.0	38.9	25.8	14.3
<i>acrD</i>	AcrAD-ToiC multidrug efflux system; permease subunit	CpxR (+), BaeR (+)	4.8	10.7	15.2	11.2	19.9	6.9		8.9	11.3	11.1	8.2	7.6
<i>marA</i>	DNA-binding transcriptional dual regulator	CpxR (+)	3.0	3.3	4.9	4.7	7.8	2.7	3.6	11.4	16.7	24.0	47.8	20.2
<i>marB</i>	Polypeptide; multiple antibiotic resistance protein	CpxR (+)		2.2			4.4	6.5		3.3	5.6	13.5	21.2	20.2
<i>marR</i>	DNA-binding transcriptional repressor	CpxR (+)				2.5	3.2			5.1	8.3	10.9	20.3	10.8
<i>mdtA</i>	Multidrug efflux system; subunit A	CpxR (+), BaeR (+)	12.4	29.3	46.3	63.2	41.8	17.1	12.4	35.2	63.0	59.9	60.2	39.3
<i>mdtB</i>	Multidrug efflux system; subunit B	CpxR (+), BaeR (+)	4.4	24.3	32.6	42.5	30.2	10.8		10.4	24.3	23.0	20.8	19.4
<i>mdtC</i>	Multidrug efflux system; subunit C	CpxR (+), BaeR (+)		9.8	24.7	24.5	24.2	8.6		7.9	22.4	28.8	21.5	17.0
<i>mdtD</i>	Predicted transport protein	CpxR (+), BaeR (+)				2.0					2.6	2.7	2.4	2.3
<i>spy</i>	Envelope stress protein	CpxR (+), BaeR (+)	34.3	124.4	357.1	330.3	420.8	250.2	14.3	200.4	585.0	605.5	672.8	656.4
<i>slf</i>	Soluble lytic murein transglycosylase	CpxR (+)		2.5	3.8	3.4	3.5	2.5		2.5	3.8	3.4	3.5	2.5
<i>degP</i>	Serine protease	CpxR (+)		2.2		7.5	7.4	4.1		2.0	16.8	18.6	23.8	12.0
<i>cpxA</i>	Sensory histidine kinase	CpxR (+)				2.0				2.0	2.9	2.8	2.1	2.5
<i>cpxP</i>	Inhibitor of the Cpx response	CpxR (+)	12.3	17.2	17.7	13.6	16.8	10.6	4.8	11.9	17.0	12.9	11.6	5.9
<i>cpxR</i>	Transcriptional dual regulator	CpxR (+)		2.3	3.4	3.2	2.6	2.0		3.1	3.4	3.4	3.3	3.1

Supp. Fig. 3 (revised)

199x264mm (300 x 300 DPI)



Supp. Fig. 4 (revised)

150x139mm (136 x 136 DPI)

	Gene	Time (min, after CORM-401 addition)					
		2.5	5	10	20	40	80
Aerobic	<i>spy</i>	34.3	124.4	357.1	330.3	420.8	250.2
	<i>uhpT</i>	3.3	18.0	78.2	124.2	216.7	142.8
	<i>mdtA</i>	12.4	29.6	48.3	83.2	41.8	17.1
	<i>baeS</i>	1.4	2.3	25.1	45.4	67.4	19.7
	<i>mdtB</i>	4.4	24.3	32.6	42.5	30.2	10.8
	<i>kdpC</i>	0.4	1.5	32.8	33.8	18.2	5.5
	<i>yhdV</i>	3.1	5.5	7.9	29.0	12.5	5.7
	<i>yebE</i>	6.6	20.7	39.8	28.9	19.7	9.4
	<i>kdpF</i>	0.9	6.2	20.8	28.0	1.8	2.0
	<i>mdtC</i>	1.0	9.8	24.7	22.5	24.2	8.6
	<i>kdpA</i>	0.9	2.9	11.3	15.6	1.5	1.5
	<i>kdpB</i>	0.7	1.3	9.8	13.8	7.5	4.8
	<i>yctS</i>	3.4	10.6	19.9	13.6	9.8	5.1
	<i>cpxP</i>	12.3	17.2	17.7	13.6	16.8	10.6
	<i>b3914</i>	9.6	17.4	18.0	13.4	15.1	10.3
	<i>cpxP</i>	9.7	17.7	18.4	12.6	16.1	10.6
	<i>yptA</i>	2.9	5.1	6.1	11.8	7.4	3.0
	<i>htpX</i>	5.1	9.2	12.7	11.7	11.7	7.4
	<i>znuA</i>	1.0	2.6	6.5	11.2	10.0	5.2
	<i>acrD</i>	4.8	10.7	15.2	11.2	10.9	6.9
	<i>chaA</i>	2.2	7.0	14.4	9.8	5.8	4.1
	<i>ybdZ</i>	1.6	4.1	4.1	9.3	2.8	2.1
	<i>metF</i>	0.9	0.0	2.4	9.0	3.7	1.0
	<i>yobB</i>	4.7	9.1	11.9	8.4	6.4	4.9
	<i>ybdZ</i>	1.7	3.8	3.5	8.3	2.0	2.0
	<i>yaaX</i>	2.9	4.2	7.5	8.3	6.3	3.3
	<i>glvC</i>	0.5	1.0	1.0	7.9	1.3	3.3
	<i>entA</i>	0.8	1.8	5.3	7.8	4.7	1.8
	<i>degP</i>	2.2	1.2	1.9	7.5	7.4	4.1
	<i>yedX</i>	2.2	6.0	4.3	7.4	5.0	4.2
Anaerobic	<i>spy</i>	14.3	200.4	585.0	505.5	672.6	556.4
	<i>uhpT</i>	1.1	8.3	39.5	112.6	112.1	106.3
	<i>mdtA</i>	12.4	35.2	63.0	59.9	60.2	39.3
	<i>baeS</i>	0.9	1.1	31.0	38.9	25.2	14.3
	<i>yebE</i>	2.4	17.2	39.1	32.0	28.0	11.6
	<i>mdtC</i>	1.0	7.9	22.4	29.8	21.5	17.0
	<i>marA</i>	3.6	11.4	16.7	28.6	47.8	20.4
	<i>mdtB</i>	1.1	10.4	24.8	23.0	20.8	18.4
	<i>marB</i>	3.3	5.6	13.9	21.7	26.7	10.3
	<i>yctS</i>	2.1	25.7	42.2	20.1	20.7	6.1
	<i>degP</i>	0.8	2.0	18.9	18.5	23.9	12.0
	<i>htpX</i>	2.4	10.5	16.1	14.5	12.5	7.6
	<i>ykgM</i>	1.5	1.2	2.5	14.3	43.3	40.9
	<i>metB</i>	1.4	1.1	5.6	13.0	2.6	0.8
	<i>cpxP</i>	4.6	11.9	17.0	12.9	11.5	5.9
	<i>b3914</i>	4.1	11.9	17.1	12.4	11.5	5.9
	<i>cpxP</i>	4.7	11.4	13.0	11.7	11.3	6.5
	<i>acrD</i>	1.9	8.9	11.3	11.1	8.2	7.6
	<i>marR</i>	1.8	5.1	8.3	10.9	20.2	10.8
	<i>metF</i>	2.0	1.2	5.9	9.8	1.5	0.7
	<i>yjflv</i>	0.6	5.9	8.2	9.6	9.2	2.1
	<i>chaA</i>	2.2	6.4	12.1	9.5	11.7	4.2
	<i>yhdV</i>	1.3	1.9	5.6	9.2	9.1	12.8
	<i>sdaA</i>	1.4	4.1	9.1	9.2	18.2	6.7
	<i>yodA</i>	0.8	1.9	3.9	9.2	34.6	15.3
	<i>mmuP</i>	1.4	1.3	3.5	8.5	1.8	1.3
	<i>metE</i>	1.4	1.1	1.9	8.1	2.1	0.5
	<i>kdpC</i>	2.8	1.4	1.3	8.0	4.6	2.8
	<i>ftmB</i>	1.4	1.5	3.1	7.9	17.8	9.7
	<i>yobB</i>	3.1	8.2	9.6	7.9	6.2	4.0

Supplementary Table 1

66x29mm (300 x 300 DPI)

Supplementary material - Open peer review of the manuscript entitled

**The Broad-Spectrum Antimicrobial Potential of $[\text{Mn}(\text{CO})_4(\text{S}_2\text{CNMe}(\text{CH}_2\text{CO}_2\text{H}))]$, a
Water-Soluble CO-Releasing Molecule (CORM-401): Intracellular Accumulation,
Transcriptomic and Statistical Analyses, and Membrane Polarization**

by

Lauren K Wareham, Samantha McLean, Ronald Begg, Namrata Rana, Salar Ali, John J Kendall,
Guido Sanguinetti, Brian E Mann, and Robert K Poole

Review comments of open reviewers:

Professor Miguel Aon
Professor Giancarlo Biagini
Professor James Imlay
Professor Nigel Robinson

Open Reviewer: Professor MIGUEL AON

Affiliation: Laboratory of Cardiovascular Science, National Institute on Aging, National Institutes of Health, Baltimore, MD 21224, U.S.A.

Email: miguel.aon@nih.gov

Section A

The work by Wareham and colleagues represents a comprehensive and in-depth assessment of the antibiotic function of CORM-401, a carbon monoxide-releasing, manganese-based compound. The most important scientific contribution of this work is the detailed assessment of the mechanism of action of CORM-401 to inhibit the growth of antibiotic-resistant bacteria, including *E. coli*, a global priority of the World Health Organization in their search for a new generation of antibiotics. The emerging picture of CORM-401 action is of a pleiotropic nature, with multiple targets that functionally converge on adverse bioenergetic effects hindering bacterial growth. Unlike the mechanism of action of current antibiotics, which generally show one highly directed and specific effect (e.g., synthesis of protein or cell wall), the CORMs represent a new generation of antibiotics that, by enabling bacteria to keep their membrane potential, favor CORMs' intracellular accumulation leading to their pleiotropic, multi-target, effects resulting in growth inhibition. In this regard, applying state of the art transcriptomics analyses, the authors show CORM-elicited significant alterations in energy metabolism- and ion transport-related gene expression, under both aerobic and anaerobic conditions.

As a former Invited Forum Editor and Author of *Antioxidant & Redox Signaling* I clearly understand and adhere to the Journal's policy of scientific excellence. In this vein, I am confident that the work by Wareham and colleagues fits those standards while making a remarkable scientific contribution.

My recommendation is to ACCEPT now that the revisions I recommended in my review report have been implemented.

Section B

The few questions/concerns raised by the Reviewers are not of enough scientific substance to reject sound work already based on a substantial and comprehensive amount of evidence. Specifically, to the critique of the lack of motility assays the authors oppose an overwhelming array of functional studies including studies of viability, metal accumulation, gene expression, respiration, membrane function, protein expression and antibiotic responses that lead to a specific proposal of a mechanism of action.

I disagree with Reviewer 2's assessment of the CORM-401 effects on respiration. In my own review of Wareham and colleagues' work, and in an otherwise sound experimental approach, I only found a few inconsistencies in their interpretation of the bioenergetic effects of CORM-401, a crucial cornerstone of their findings leading to the mechanism of action of this compound. The authors were able to handle them easily and to my satisfaction. The key issue to be understood from this work is that the perturbations of the proton motive force elicited by CORM-401 are matched by enhanced respiration leading to membrane polarization, which in turn drives the uptake of CORM-401 by bacteria, poisoning them by its intracellular accumulation. This seminal effect facilitates the intracellular action of CORM-401 on multiple targets leading to growth arrest.

Conflict of Interest Disclosure

I have no personal interest or involvement in this work, and I have not collaborated with any of the authors of this study.

Open Reviewer: Professor GIANCARLO BIAGINI

Affiliation: Liverpool School of Hygiene and Tropical Medicine, Liverpool
L3 5QA, UK

Email: giancarlo.biagini@lstmed.ac.uk

Section A

The manuscript investigates the mechanism of action of a CO-releasing molecule [Mn(CO)₄(S₂CNMe(CH₂CO₂H))], CORM-401, which is a Mn-based carbonyl complex compared to the first generation ruthenium-based carbonyl complexes. The study describes biochemical, cellular bioenergetic and transcriptional responses of *E. coli* to CORM401. The innovation of the manuscript is that these data are the first to describe the pharmacodynamics of this “second generation” CORM-401. The findings suggest a pleiotropic mechanism of action, which includes disruption of respiratory chain components and of membrane integrity, in terms of ion transport/homeostasis. It is likely that the disruption of these two biological functions is linked. Transcriptional data support these observations and suggest a bacterial stress/repair response to overcome these inhibitory effects. The data are robust but I would have liked to see further investigations into the cellular bioenergetics for example determining whether the uncoupler effect led to a disruption in transmembrane pH and to determine whether the uncoupler effect is at all linked to uncoupler-stimulated ATPase activity. In terms of therapeutic potential, CORM-401 represents a new class of antibacterial but anti-proliferative effects are modest and data do not show any synergy with other antibiotics used – the authors should remove from the abstract that CORM401 potentiates with cefotaxime and trimethoprim as the authors have correctly stated in the manuscript that the effect is additive – potentiation is a distinct phenomenon.

Addressing the above suggestions/comments I would RECOMMEND FOR PUBLICATION.

Section B

Reviewer objections following additional experiments include the following;

“[Lack of] functional studies have been proposed” –

Respectfully, I would argue that the authors have extensive functional pharmacodynamic data. The pleiotropic mechanism of action, very common with inhibitors of this kind, means that there is no one simple functional assay/phenotype. The observed inhibitor profiling of CORM-401 using biochemical and cellular bioenergetic assays links an inhibition of the respiratory chain to a disruption of the ionic potential. I have commented on some additional assays that could be carried out e.g. monitoring of pH and ATPase activity – *but it should be noted that this manuscript already contains a very high volume of data.* The authors are perhaps guilty of not providing an hypothesis linking the observations, but this could be requested.

One of the referees questions the demonstration that CORM-401 stimulates respiration. However, I would respectfully argue that this is clearly demonstrated in Fig 7. The experiments show the use of the open O₂ electrode, widely used and often in preference to the closed system as one has the ability to set the dissolved O₂ tension of the chamber, which clearly demonstrates stimulation of O₂ consumption following the introduction of CORM-401. The positive control experiment using KCN clearly indicates that the system is working normally.

The ‘lack of in vivo studies is a major concern’.

In vivo data are required in order to establish the develop potential of molecules but, in this case, this investigation is first attempting to determine the molecular mechanisms underpinning the activity of this class of compounds. It is therefore not normal practice to conflate the two issues.

1
2
3
4
5
6
7
8
9
10
11
12
13
14
15
16
17
18
19
20
21
22
23
24
25
26
27
28
29
30
31
32
33
34
35
36
37
38
39
40
41
42
43
44
45
46
47
48
49
50
51
52
53
54
55
56
57
58
59
60

Conflict of Interest Disclosure

I have no personal interest or involvement in this work, and I have not collaborated with any of the authors of this study.

Open Reviewer: Professor JAMES A IMLAY

Affiliation: Department of Microbiology, University of Illinois, Urbana, IL 61801, U.S.A.

Email: jimlay@illinois.edu

Section A.

I have closely read the manuscript and the reviewers' comments. My overall reaction is that the manuscript is sound, and I advise that a decision be made to ACCEPT the paper. Reviewer 1 made a couple of suggestions that would expand the scope (motility, in vivo experiments), but for the reasons below I do not think these are advisable. Because CORMs affect mammalian cells, it is premature (from both analytical and safety viewpoints) to engage in animal experiments as an add-on to a basic mechanistic study.

Reviewer 2 is unfamiliar with the use of steady-state rather than direct consumption measurements, as a means of tracking respiration. Part of that reviewer's concern appears to stem from the thought that *E. coli* might consume oxygen through non-respiratory routes. As explained below, I can vouch that this is not the case, based on our own measurements of oxygen consumption and ROS production. This view is uncontroversial in the *E. coli* community.

Aside from the reviewers' comments, I'll add that I was surprised by the outcome. I would have predicted that toxicity was mediated by the usual action of CO. The loss of viability in Fig. 2 was enough to alert me that I was wrong. This is nice work.

Section B.

Point-by-point comments in response to reviewers' concerns:

Motility..... Motility assays would be confounded when CORM-401 disrupts the membrane potential, which powers motility. Most bacteriostatic stresses block motility. I regard this experiment as unnecessary.

in vivo analysis..... Because these compounds impact host cells, a study of CORM-401 impact in host animals would be large and complex.

It is very likely that there are more bacilli in the chamber at point 2..... In glucose/buffer, cells will not grow (due to the abrupt removal of nutrients). This concern is unfounded.

Instead of total oxygen level – Authors should determine O₂ consumption rate (OCR), This method is not new. Standard measurements of consumption (Fig. 7B) are problematic when rates are low. But in Figs. 7C and 7D the reader can immediately see that CORM-401 and CCCP cause an increase in oxygen consumption, as evidenced by the lower steady-state oxygen level. (Similarly, in natural bacterial habitats any acceleration of respiration shifts ambient oxygen levels to a lower steady-state. This experiment recapitulates that effect.)

..... it is difficult how low O₂ tension would affect respiration in the presence of CORM.

The hypothesis is that CO competitively inhibits oxygen consumption. If true, CO would inhibit most when the competing substrate—molecular oxygen—is scarce. Thus the low-oxygen set-up amplifies the response. Indeed, a second bolus of CORM-401 raised the steady-state oxygen concentration.

Secondly, oxygen consumption or even OCR could increase due to several processes other than respiration. I disagree with the reviewer's suggestion that non-respiratory processes could accelerate oxygen consumption. *E. coli* lacks non-respiratory enzymes that employ molecular oxygen as a substrate, as this facultative bacterium must manage biosynthesis without oxygenases. Trace oxygen consumption

1
2
3
4
5
6
7
8
9
10
11
12
13
14
15
16
17
18
19
20
21
22
23
24
25
26
27
28
29
30
31
32
33
34
35
36
37
38
39
40
41
42
43
44
45
46
47
48
49
50
51
52
53
54
55
56
57
58
59
60

occurs via ROS formation, but measurements show this rate is < 1% of the respiratory rate. Indeed, if one knocks out the respiratory oxidases, oxygen consumption essentially ceases.

Conflict of Interest Disclosure

I have no personal interest or involvement in this work, and I have not collaborated with any of the authors of this study.

CONFIDENTIAL. For Peer Review Only

Open Reviewer: Professor NIGEL ROBINSON

Affiliation: Department of Biosciences, Durham University, Durham, DH1 3LE, U.K.

Email: nigel.robinson@durham.ac.uk

Section A

It has been suggested that carbon monoxide releasing molecules (CORMs) might be exploited as a new class of antimicrobials, with the looming threat of antimicrobial resistance making work to explore such options pertinent. We learn here that growth inhibition by CORM-401 correlates with the accumulation of its integral manganese. Manganese itself is typically considered to be an antioxidant rather than a pro-oxidant. Redox active metals such as iron and copper drive the Fenton reaction to generate deadly hydroxyl radicals while manganese can act as a functional superoxide dismutase even in the absence of an associated protein, for example as observed in radiation-resistant *Deinococcus radiodurans*, which accumulates vast amounts of protective non-protein-bound manganese. The CORM-401-associated manganese predominantly accumulates in the cytosol with a substantial amount also associated with DNA, and some aspect of its localization or chemical context must engender toxicity. It was anticipated that the basis of bacterial toxicity of CORM-401 would be via the released CO and in turn the liberated CO would target heme molecules and in consequence bacterial respiration. Here, multiple approaches have explored various facets of bacterial physiology (respiration, transport, membrane integrity) and molecular cell biology (including extensive expression profiling) to carefully tease apart the mechanism(s) of bacterial growth inhibition by CORM-401. The resulting observations do not mirror the effects of related ruthenium-containing CORMs, neither does exposure of cells to CO alone mimic the effects of CORM-401: these data thus point to features of the compound other than solely the liberated CO exerting inhibitory effects, with manganese as opposed to ruthenium, appearing to be one crucial distinction. The work is a *tour de force*, but perhaps its breadth and scope have (up to now) been one of its failings in that the story does not follow a single simple path. Multiple avenues are explored to create a more complete and unbiased picture of the physiological effects of CORM-401. In short, the action of CORM-401 is multifaceted and includes CO-binding to respiratory oxidases but also manganese hyper-accumulation with effects on the homeostasis of other metals (such as zinc), ionic imbalance and loss of membrane integrity, plus crucially specific effects on defined regulons. There was scope to make the narrative more accessible to the general reader, but these extensive data need to be in the public domain.

Section B

First Referee: The extent of functional studies is questioned. The work is rich in a diversity of types of functional studies including analyses of cell viability, metal accumulation, gene expression, respiration, membrane function, protein expression and antibiotic responses. These assays have demanded a high degree of technical skill in using a wide range of methodologies. The referee has specifically criticised the lack of motility assays but seems to have ignored the broad range of studies that are present. Nonetheless, it seems that the authors could relatively swiftly complete some motility studies, and revise the manuscript accordingly, with a minimum of fuss-and-bother and in so doing meet a residual concern of this referee.

Second referee: Evidence that the compound stimulates respiration is questioned. However, bacterial respiration rates have been determined from measurements of both oxygen concentrations and of oxygen diffusion rates, common approaches in, for example, biochemical engineering (see Fig. 7). The senior author is a long-standing member of a relatively small cohort of aficionados of bacterial respiration. Perhaps the referee is more familiar with different types of measures of eukaryotic respiration.

1
2
3
4
5
6
7
8
9
10
11
12
13
14
15
16
17
18
19
20
21
22
23
24
25
26
27
28
29
30
31
32
33
34
35
36
37
38
39
40
41
42
43
44
45
46
47
48
49
50
51
52
53
54
55
56
57
58
59
60

Editorial comments note the lack of *in vivo* studies. Extensive studies in living bacterial cells are described here. However, in this context it may be felt that ultimately the compound should be used in animal models of infection. An outcome of this work has been to highlight the novel mode(s) of action of CORM-401, which now suggest several routes for the development of more effective antimicrobials. However, the modest effectiveness of this particular CORM as an antimicrobial agent suggests that animal studies are not justified (or perhaps ethical) for this particular compound.

The overall recommendation was to REVISE the manuscript to include the requested motility studies and also to improve the narrative as noted previously. Also, the manganese content of cells is given as a concentration and my preference would be to express these data as atoms/ions per cell (the number of cells per unit cell mass should be easy to determine). This is because most of the accumulated manganese will be bound and buffered such that the exchangeable concentration within living cells will be much lower than these values suggest. These changes have now been made.

Conflict of Interest Disclosure

I have no personal interest or involvement in this work, and I have not collaborated with any of the authors of this study.

20 June and 11 July 2017

Dear Dr Sen

Manuscript ID ARS-2016-6971 (now) entitled " The Broad-Spectrum Antimicrobial Potential of [Mn(CO)₄(S₂CNMe(CH₂CO₂H))], a Water-Soluble CO-Releasing Molecule (CORM-401): Intracellular Accumulation, Transcriptomic and Statistical Analyses, and Membrane Polarisation", submitted to *Antioxidants & Redox Signaling*.

Your response of 27 December 2016 to our first submission indicated that all reviewers expressed some enthusiasm for our work and one recommended outright acceptance. We acted on the recommendations in all the reports we received in full and spent three months on further experiments, recruiting extra staff to the many tasks.

After our second submission we received on 22 May two sets of comments together with your decision to reject our manuscript. This was despite the fact that neither of the reviewers was damning in their assessment and our numerous improvements were acknowledged. Feeling that we had been unfairly treated, for reasons to be expanded up below, I wrote to you on 23 May expressing our dissatisfaction and disappointment. Your response on 25 May, for which we thank you, stated:

"If you are willing to add substantial in vivo (preferably mammal, more relevant to human health in this context) data, ARS would be willing to reconsider this work. Time limits can be flexible. As it relates to ethical or scientific justification, for work intended to 'open the way for new compound design and novel clinical, combinatorial therapies' we believe that work testing in vivo efficacy and mechanisms are justified. At the same time we acknowledge that there may be justifiable differences in opinion on this matter. In the absence of such in vivo data, ARS offers the REBOUND TRACK for all authors unhappy with their REJECT decision."

Having consulted with colleagues, we have decided to use the REBOUND TRACK and now submit a third version, together with reports from 4 independent open peer reviewers, as directed. They are:

1. Miguel Aon (National Institute on Aging (NIH), USA) – mitochondrial energetics
2. Giancarlo Biagini (Liverpool School of Tropical Medicine, UK) – parasitology; antimicrobial agents
3. James Imlay (University of Illinois, USA) - Molecular mechanisms of oxidative damage; cellular defenses against oxidants
4. Nigel Robinson (University of Durham, UK) – metal ions in biology; bacterial physiology

In reviewing the publication records of these open reviewers, we respectfully ask you to note that no journal in the field of Microbiology (except *Nature*) has an Impact Factor equalling ARS. It is widely held, I believe, that *Molecular Microbiology* is the top specialist journal in our field. We point out that we hold other equally favourable reviews from several other scientists that we have approached and we are happy to share these.

Please note that this version includes the open peer reviews in Supplementary Text as required by the online Instructions to Authors AND condensed comments inserted in shaded boxes in the text (pp. 5-11) as illustrated in samples provided by Ms Khanna and you.

1
2
3
4
5
6
7
8
9
10
11
12
13
14
15
16
17
18
19
20
21
22
23
24
25
26
27
28
29
30
31
32
33
34
35
36
37
38
39
40
41
42
43
44
45
46
47
48
49
50
51
52
53
54
55
56
57
58
59
60

In the light of correspondence with our open reviewers and with other colleagues whose reports are not included here, we have performed some further experiments, and comprehensively responded to the concerns, both in the manuscript and in this covering letter.

We therefore submit a revised manuscript that we ask you to reconsider. Kindly note that the reviewers' comments, where reproduced, are in *italics*. Our responses are in **bold**. Because of the substantial changes requested in previous submissions, the comprehensive nature of the datasets, and the need for new experiments and their description, this submission is necessarily longer than the original.

In addition to the points raised variously by the two reviewers and four open reviewers, we have made the following changes to this third version.

- minor title change to clarify the effects on the membrane
- improvement of the Conclusions in Abstract and of the term 'potentiates' in favour of 'enhances'
- clarification of the meaning of intracellular metal levels in response to a helpful comment by Professor Robinson (p. 12)
- a major increase in our explanation of the open electrode method (pp. 18-21)
- much improved text on the membrane polarisation (Fig 8) (pp. 21-22)
- new motility assays (p. 26-27)
- removal of the antibiotic data to Supplementary material, leaving a vacancy for a hypothetical diagram (new Fig 14) as requested by reviewers
- improved clarity of the narrative to aid the general reader
- changes in emphasis in the Discussion to reflect reviewers' suggestions and relegate the importance of the antibiotic data
- new Methods and references to support the above

In conclusion, we believe that this extremely thorough revision now addresses the points raised by the two previous reviewers and the four open reviewers. We submit this revised manuscript and ask you to reconsider it in the light of the above responses.

Robert K Poole
(For the authors)

Reviewer: 1 Comments to the Author

The revised manuscript from Wareham et al. includes additional material concerning the extent to which CORM-401 compound has broad-spectrum antibiotic activities. Several points from my previous reviewing:

to multiply the number of strains, and possibly use clinically relevant strains: Authors have taken into consideration this comment and have used, in addition to initial strain of E. coli, other members of Enterobacteriaceae: Klebsiella, Shigella, Salmonella, Enterobacter, and Citrobacter but also Pseudomonadales (Pseudomonas and Acinetobacter). Interestingly, authors have also investigated antibiotic efficacy of CORM-401 using an antibiotic-resistant clinical strain of E. coli (EC958). Using that collection of microbes, CORM-401 appears to have broad-spectrum activities for Enterobacteriaceae, while no effects were reported on Pseudomonadales.

Noted

No functional assays have been proposed to complement the transcriptomic analysis presented (e.g. motility assays). I still think this would be important addition.

The open reviewers are unanimous in their views that the numerous data we present on gene viability, expression, metal accumulation, respiration, membrane polarisation etc. ARE functional assays in the context of microbes. Nevertheless we now include motility assays as requested as well as a section in Methods. As we anticipated, these data do not significantly increase the value of the manuscript.

No in vivo study has been performed in this re-submission, I keep this recommendation for future investigations.

This reviewer appears no longer to require these data in an animal model, yet your letter requests them. The open reviewers are unanimous in their views that it is premature to perform animal experiments given the relatively modest antimicrobial effects *in vitro*.

I still think that some figures are difficult to read. Histograms like in Figure 2 and Figure 13 would benefit from using a legend box to help readers.

We have added explanatory labels to Figs 7 and 8.

Authors included new discussions regarding CORM-401 toxicity towards eukaryotic cells, and included appropriate references.

Noted

I appreciated the several editing improvements in the text compared to previous version. Several experiments were included in response to other reviewers' questions.

Noted

This revision brings new improvement in the text and in the scientific content over the previous submission.

Noted

Reviewer: 2 Comments to the Author

I have following comments on this revised submission:

Page 15 -line 43-49- the conclusion drawn from Fig 7C is that - CORM stimulated the respiration (>2 fold). I am intrigued by this conclusion. In Fig 7C, from point 1 to point 2, in roughly ~20 min, O₂ consumption is ~375-400 mmoles. Following CORM addition (at point 2), approximately 200 m moles of O₂ is consumed in ~ 20 min or so (which is roughly 45-50% of O₂ consumed from point 1 up to point 2). It is very likely that there are more bacilli in the chamber at point 2, than they were at point 1 considering the doubling time of E coli is relatively short ~20-25 min. overall, more bacilli accounted for a lesser reduction in oxygen levels, which is in contrast with the conclusion that CORM401 stimulates respiration. Can authors comment on that?

This comment and those that follow on respiration were made after submission of the second version but not the first. We find this unfair and so do some of the reviewers, since the respiration data are identical in versions 1 and 2. It is clear that this reviewer is wrong: we show in Fig. 7B-D nmoles (nmol) NOT mmoles (millimol). It is physically impossible to consume “~375-400 mmoles” since oxygen solubility is only c. 200 micromolar!

Instead of total oxygen level – Authors should determine O₂ consumption rate (OCR), which would be a better and accurate indicator to measure the effect on oxygen consumption and also account for the bacterial growth during the process of experiment. This should be doable since O₂ diffusion constant is known that authors use to claim a ~2 fold increase in respiration (?).

We must conclude that this reviewer simply does not understand the steady state method in an open electrode vessel for measuring respiration. It has been in use since 1973 (see reference 10). To avoid any confusion in the minds of other readers, we have extensively expanded the explanation of the method and provided actual rates of oxygen consumption.

With the scale used for Fig 7D and without knowing actual basal E coli OCR, it is difficult how low O₂ tension would affect respiration in the presence of CORM.

We do not understand this comment; one open reviewer has correctly stated that the experiment in Fig 7D was designed to study the effects of the CORM at very low oxygen tensions in the chamber. The open reviewers support our argument.

Can authors comment on the effect on OCR following addition of CORM twice for exp in Fig 7C as they did for experiment in Fig 7D?

We see no need for a second CORM application in Fig 7C when the effects of the first application are so clear-cut.

Throughout the manuscript, authors claim that CORM stimulates respiration (like in page 16-line 13 line 53-54, page 25, discussion, and elsewhere). However, authors have essentially measured only oxygen levels following exposure to CORM. The author claims a 2-fold increase in basal respiration rate/without any data plotting and comparing E coli OCR following 1uM of CCCP addition (line 53-54, page 25). Secondly, oxygen consumption or even OCR could increase due to several processes other than respiration. In the absence of any ATP measurements/bio-energetic assays, the conclusions about respiration rate are not valid.

The reviewer is mistaken in stating that “we have essentially measured only oxygen levels following exposure to CORM”. This is simply incorrect. In conjunction with the oxygen level, we

1
2 have measured oxygen transfer rates, so that oxygen consumption rates can be calculated. See
3 reference 10. It is absolutely clear that CORM-401 stimulates bacterial respiration. The
4 comments of this reviewer should be discounted as grounds for rejection. Again the open
5 reviewers support our case.
6
7
8
9
10
11
12
13
14
15
16
17
18
19
20
21
22
23
24
25
26
27
28
29
30
31
32
33
34
35
36
37
38
39
40
41
42
43
44
45
46
47
48
49
50
51
52
53
54
55
56
57
58
59
60